Metadata of the chapter that will be visualized in SpringerLink

Book Title	Cognitive Radio Policy and Regulation	
Series Title	4748	
Chapter Title	Technical Approaches for Improved Spectrum Sharing	
Copyright Year	2014	
Copyright HolderName	Springer International Publishing Switzerland	
Corresponding Author	Family Name	**Velez**
	Particle	
	Given Name	**Fernando J.**
	Suffix	
	Division	
	Organization	UBI - Instituto de Telecomunicações
	Address	Aveiro, Portugal
	Email	fjv@ubi.pt
Author	Family Name	**Matinmikko**
	Particle	
	Given Name	**Marja**
	Suffix	
	Division	
	Organization	UBI - Instituto de Telecomunicações
	Address	Aveiro, Portugal
	Email	Marja.Matinmikko@vtt.fi

Abstract

The aim of this chapter is to showcase several important contributions towards identification of techniques for spectrum sharing and coexistence. It is envisaged that such novel techniques may be of value in various regulatory considerations. They might assist in shaping technical conditions that will govern the access to radio spectrum by CR technologies. Section 3.1 reviews the recommended principles of Geolocation Databases' operation in European regulatory environment, as well as the envisaged structural composition of technical solutions for their implementation. Section 3.2 is composed of several contributions that offer different angles of looking at CR spectrum sensing algorithms and implementation techniques. It also considers the possibilities of dynamic re-configurability through beam forming capabilities. This is followed by discussion in Sect. 3.3 of possibilities for spectrum aggregation from non-contiguous frequency bands, as made possible by the DSA capabilities of CR. This opens up possibilities for significantly increasing the available operational bandwidth—and hence the data throughput—of the radio transceivers. It also allows pursuing energy efficiency objectives. Section 3.4 looks at the possibilities of developing unsynchronised CR networks using Filter Bank Multi-Carrier, an alternative type of modulation that offers a superior performance and reduced out-of-band emissions compared with other traditional types of modulation. The detection of malicious users is addressed in Sect. 3.5, by employing a statistical approach. This approach allows reliable detection of users even when the system does not have a priori information about primary channel activity and characteristics of users. The following Sect. 3.6 looks at the spectral efficiency of CR systems and the related possibilities of using Iterative Water-filling method, which may be highly beneficial for broadband wireless channels under static or slowly varying conditions. The final Sect. 3.7 contains two contributions that present different aspects associated with the issue of assessing the amount of white spaces, or in other words—spectrum resource available for DSA access. It first looks at the principles of Radio Environment Mapping, which is then complemented by an example of evaluating amount of TV band white spaces in Italy.

Layout: T1 Standard SC | Book ID: 318863_1_En | Book ISBN: 978-3-319-04021-9
Chapter No.: 3 | Date: 24-12-2013 | Page: 1/60

Chapter 3
Technical Approaches for Improved Spectrum Sharing

Fernando J. Velez and Marja Matinmikko

Abstract The aim of this chapter is to showcase several important contributions towards identification of techniques for spectrum sharing and coexistence. It is envisaged that such novel techniques may be of value in various regulatory considerations. They might assist in shaping technical conditions that will govern the access to radio spectrum by CR technologies. Section 3.1 reviews the recommended principles of Geolocation Databases' operation in European regulatory environment, as well as the envisaged structural composition of technical solutions for their implementation. Section 3.2 is composed of several contributions that offer different angles of looking at CR spectrum sensing algorithms and implementation techniques. It also considers the possibilities of dynamic re-configurability through beam forming capabilities. This is followed by discussion in Sect. 3.3 of possibilities for spectrum aggregation from non-contiguous frequency bands, as made possible by the DSA capabilities of CR. This opens up possibilities for significantly increasing the available operational bandwidth—and hence the data throughput—of the radio transceivers. It also allows pursuing energy efficiency objectives. Section 3.4 looks at the possibilities of developing unsynchronised CR networks using Filter Bank Multi-Carrier, an alternative type of modulation that offers a superior performance and reduced out-of-band emissions compared with other traditional types of modulation. The detection of malicious users is addressed in Sect. 3.5, by employing a statistical approach. This approach allows reliable detection of users even when the system does not have a priori information about primary channel activity and characteristics of users. The following Sect. 3.6 looks at the spectral efficiency of CR systems and the related possibilities of using Iterative Water-filling method, which may be highly beneficial for broadband wireless channels under static or slowly varying conditions. The final

F. J. Velez (✉) · M. Matinmikko
UBI - Instituto de Telecomunicações, Aveiro, Portugal
e-mail: fjv@ubi.pt

M. Matinmikko
e-mail: Marja.Matinmikko@vtt.fi

A. Medeisis and O. Holland (eds.), *Cognitive Radio Policy and Regulation*, Signals and Communication Technology, DOI: 10.1007/978-3-319-04022-6_3,

Layout: T1 Standard SC | Book ID: 318863_1_En | Book ISBN: 978-3-319-04021-9
Chapter No.: 3 | Date: 24-12-2013 | Page: 2/60

Sect. 3.7 contains two contributions that present different aspects associated with the issue of assessing the amount of white spaces, or in other words—spectrum resource available for DSA access. It first looks at the principles of Radio Environment Mapping, which is then complemented by an example of evaluating amount of TV band white spaces in Italy.

3.1 Geo-Location Databases

Alexander Kholod

Federal Office for Communications, Biel/Bienne, Switzerland
e-mail: alexandre.kholod@bakom.admin.ch

3.1.1 Background

An important issue when getting the access to spectrum by a cognitive radio system [1] is the protection of incumbent users of this spectrum. The geo-location database is one of the cognitive techniques used to assess the current usage of the spectrum and to assist accessing this spectrum without placing undue constraints on incumbent users of the spectrum.

The principles and requirements to the cognitive technique employing the geo-location database were developed in the course of the CEPT studies on white space devices (WSDs). WSDs are defined as devices that can utilise White Space spectrum[1] without generating harmful interference to incumbent services by making use of cognitive techniques.

To this end, ECC Report 159 [3] sets initial principles and operation requirements to WSDs under the geo-location database technique, which are further developed in ECC Report 186 [4].

3.1.2 Introduction

An increased interest to the geo-location technique is outlined by its flexibility and scalability in addressing various cognitive wireless systems: from local television WSDs [3] to industrial level geo-location solutions to support Licensed Shared Access operations of cellular mobile networks [5].

[1] *White Space spectrum is defined by the CEPT* [2] *as "a label indicating a part of the spectrum, which is available for a radio communication application (service, system) at a given time in a given geographical area on a non-interfering/non-protected basis with regard to other services with a higher priority on a national basis".*

Layout: T1 Standard SC | Book ID: 318863_1_En | Book ISBN: 978-3-319-04021-9
Chapter No.: 3 | Date: 24-12-2013 | Page: 3/60

Though the concept of White Space spectrum was first used in connection to the band 470–790 MHz, it can be translated to other frequency bands, which are considered underutilized either in terms of location or time. Furthermore, the principles for the geo-location database operation are generic and can be considered without application to a particular frequency band and related protection of a particular incumbent user.

This section presents the general concept of the geo-location database operation and discusses different issues in this regard. The requirements to two integral parts of the geo-location database system, namely the database and the WSD, are considered as well.

3.1.3 General Principles

The geo-location technique is the process, where a WSD measures its geographical location and queries a geo-location database in order to get information on available frequencies at this location. As discussed later in this section this process requires some exchange of information to occur between the WSD and the geo-location database.

The determination accuracy of the WSD geographic location is one of the crucial elements in the whole process. In particular, any errors in location determination may alter the fundamental purpose of using the geo-location database, which consists in ensuring the operation of incumbent users free from WSD interference. The WSD should maintain this accuracy while in operation.

A closely related aspect is the mesh used by the geo-location database to store information on spectrum usage across a given geographical area. Under a large scaled mesh, the information on spectrum availability might be inaccurate. Too fine mesh will likely result in elevated computing efforts and an increased data transfer.

3.1.3.1 Master-Slave Concept

A radio communication link between the devices of the same application will always involve at a minimum two transmitting/receiving units. Therefore, any operational scenario with WSDs can be described as a communication between a master device and a slave device.

A master WSDs is a WSD that can establish a direct communication channel with a geo-location database to obtain operational parameters pertinent to its geographical location. A slave WSDs cannot establish such a communication channel and obtains the relevant operational information directly from its serving master WSD.

To this end, one distinguishes between two cases of master/slave WSD deployment: one for so-called non-geo-located slaves and another for geo-located slaves. Both cases are illustrated schematically in Fig. 3.1.

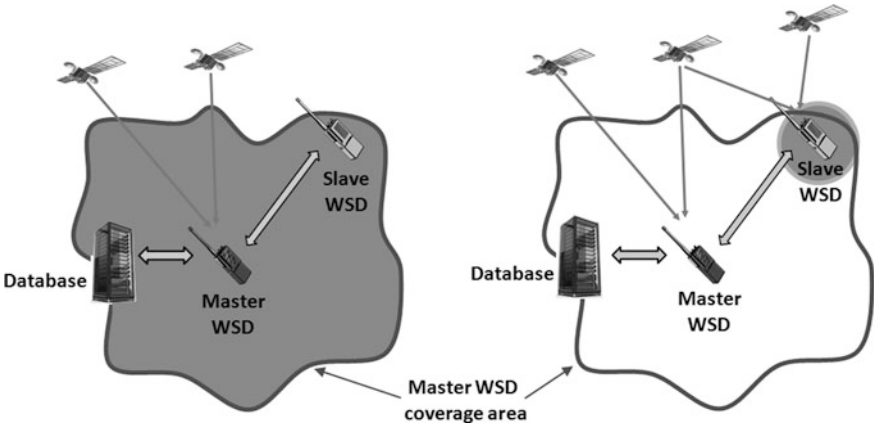

Fig. 3.1 Master/slave concept with non-geo-located (*left*) and geo-located (*right*) WSDs. The *shadow regions* show the area, within which the slave WSDs can be determined to be located

In the case of non-geo-located slaves, the master does not know the exact geographical locations of the slaves within its coverage area. Therefore, the operational information obtained by the master WSD from the database and communicated further to the slave WSDs is valid for the whole coverage area of the master WSD. The coverage area can be determined either by the master WSD itself or by the geo-location database on the basis of information received from the master.

In the case of geo-located slaves, the master knows the exact geographical locations of its slaves. It queries, therefore, the database for its own operational parameters and then sequentially for each slave. The received information is then communicated to appropriate slaves.

The requirements set to the geo-location database operation are differentiating between those applied for master WSDs and those applied for slave WSDs.

3.1.3.2 Technical and Operational Requirements

The baseline for the transmission allowance for master WSDs in the territory of a country is the discovery of a geo-location database, which has been approved by the regulator of that country. This requirement is sometimes called 'no-go requirement'. If it is met successfully, an exchange of information between the master WSD and the geo-location database as well as between the master WSD and the slave WSDs will need to take place.

In particular, the master WSD shall communicate to the database its device parameters including the geographical location, the accuracy this location has been measured, device type (fixed installation or portable/mobile), device emission characteristics (e.g. spectrum mask, emission technology, etc.), device model (to enable solving interference problems), device unique identifier (to allow tracing individual devices) and device category (master or slave). The master

Layout: T1 Standard SC | Book ID: 318863_1_En | Book ISBN: 978-3-319-04021-9
Chapter No.: 3 | Date: 24-12-2013 | Page: 5/60

WSD shall also communicate to the database the device parameters of its associated slaves. The master WSD may optionally communicate to the database the detailed antenna characteristics, including the antenna height, antenna angular discrimination, and antenna polarisation, for itself and associated slave WSDs provided such information is available.

The geo-location database will then communicate back to the master WSD the list of available frequencies within the device's location (for both the master and slaves WSDs), the associated maximum permitted transmit power levels for each of available frequencies, and the validity time of parameters provided. The geo-location database may optionally communicate to the master WSD a sensing threshold for the detection of incumbent services as well as a so-called "cease operation" message that can be used in exceptional cases to request the master WSD and its associated slave WSDs to stop instantaneously their transmissions.

It stands to reason that the master WSD shall only operate in accordance with the above technical and operational parameters received from the geo-location database. The following needs to be added here. After having received the above instructions from the geo-location database and before commencing any transmission, the master WSDs shall communicate to the database the channel usage parameters, which include the selected frequency, intended transmit power and, optionally, its coverage area (in case of non-geo-located slave WSDs). These parameters will be used by the database to assess the spectrum usage by WSDs in a given geographical area and, if required, take account of cumulative interference.

In a similar way as it is done between the master WSD and the geo-location database, the slave WSD shall communicate to its serving master WSD the list of device parameters that includes the device type, device emission characteristics, device model and device unique identifier. For the geo-located slave WSDs, the list of device parameters sent to the database will also include the slave WSD antenna location and the antenna location accuracy. Optionally, the detailed antenna characteristics may also be communicated by the slave WSD to its serving master WSD.

The slave WSD shall be capable of receiving from the master WSD the information on available frequencies, the associated maximum permitted transmit power levels, and the validity time of parameters provided. Optionally, the master WSD may send to its slave WSD a sensing threshold for the detection of incumbent services as well as the "cease operation" message. The slave WSD may only operate in accordance with the instructions received from the master WSD. It shall stop immediately its transmission if instructed to do so by its serving master WSD or when no communication with the master WSD can be established after the validity time.

3.1.3.3 Combined Sensing and Geo-Location

It is also possible to combine the geo-location database technique with the spectrum sensing. Such a combined technique presents two potential advances compared to the geo-location database only; however, these advances appear to be mutually exclusive.

Layout: T1 Standard SC | Book ID: 318863_1_En | Book ISBN: 978-3-319-04021-9
Chapter No.: 3 | Date: 24-12-2013 | Page: 6/60

One benefit consists in the improved detection of incumbent users of the spectrum compared to the cases when either spectrum sensing alone or geo-location database alone are used. A favorite decision on the spectrum availability is taken only when both the geo-location database and the spectrum sensing confirm the absence of an incumbent spectrum user at the WSD location.

Another benefit is that the combined technique may also allow the detection of incumbent spectrum users, which are not registered in the database. In particular, such incumbent users are detected by means of the spectrum sensing without support with information from the database. The combined detection and associated decision is only then employed for the incumbent users, which are registered in the database.

It needs to be mentioned here that the implementation of reliable spectrum sensing has a number of challenges [6]. Therefore, the potential benefits of the combined approach mentioned above may not be achievable in practice.

3.1.3.4 Database Management Issues

A general approach to the geo-location database management is presented in Fig. 3.2. The goal of this process is to ensure protection of incumbent users of the spectrum while providing WSDs with access to this spectrum. There are a number of key elements associated with the geo-location database management.

In order to ensure protection of incumbent users of the spectrum, the database should be loaded with the information on these users. This could be achieved by recording transmitter parameters (like antenna location, height and pattern, output power, etc.) and receiver characteristics (like sensitivity level, protection requirements, etc.) for each of the protected services/systems. Another possibility could be to associate each point of the database mesh with the received signal characteristics of the incumbent users.

The database is to contain the latest information on incumbent users. An important parameter in this regard is the database update delay, which defines the time period set to update the database once incumbent users provide a notice of a change in their assignments. Another important parameter related to the information on incumbent users is the database update frequency. This parameter sets the periodicity of database update required to keep the information in the database valid.

The information received by the database from the WSD and the information contained in the database on incumbent spectrum users would have to be converted into the list of available frequencies at the WSD location and associated maximum permitted transmit power levels for each of available frequency. Hence, a translation process is to be performed to bridge these two ends. This is a critical element in the whole geo-location database architecture indeed and is to be implemented properly. If it is not, there is a risk either of interference into incumbent users, or of the WSD access to the spectrum being limited without cause.

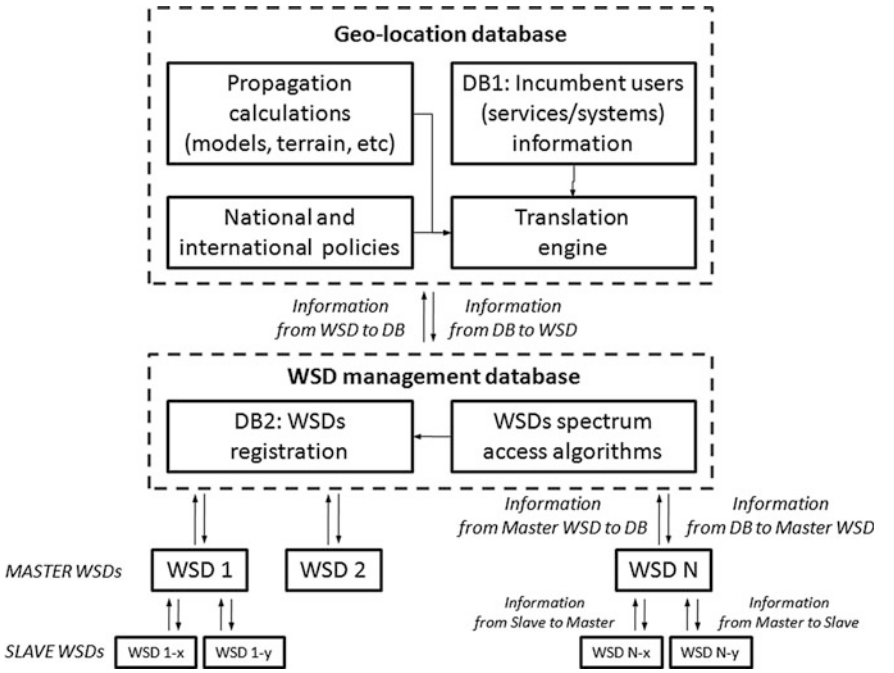

Fig. 3.2 Geo-location database management

The algorithms implementing the translation process depend primarily on the type of the incumbent service/system. Propagation loss calculations constitute an inherent part of these algorithms. It needs to be highlighted here that the way the translation process is implemented must be in conformity with related national and international policies. In particular, international policies cover the cases when a WSD in one country could potentially interfere harmfully with an incumbent spectrum user in a neighbouring country.

More than one WSD may seek for spectrum access in a given geographical area. In order to ensure that different WSDs access the spectrum in a coordinated manner (e.g. without mutual interference) special spectrum access algorithms need to be implemented. These algorithms are also governed by national policies with regard to spectrum sharing between WSDs and incumbent users and between WSDs themselves.

Furthermore, the WSDs that were already granted spectrum access need to be registered in the database. This would help the geo-location database to correctly assess and coordinate the spectrum usage by WSDs in a given geographical area. The knowledge about WSDs operating in the area is also required in order to consider properly cumulative interference from WSDs into incumbent spectrum users.

Layout: T1 Standard SC | Book ID: 318863_1_En | Book ISBN: 978-3-319-04021-9
Chapter No.: 3 | Date: 24-12-2013 | Page: 8/60

3.1.4 Concluding Remarks

The geo-location technique is a powerful tool to ensure a controlled access to underutilized spectrum. Development of a regulatory framework for this technique raises some issues and sets a number of requirements. The treatment of these issues and the implementation of these requirements require coordinated efforts by both the regulatory and standardization organizations.

3.2 Cooperative CR Spectrum Sensing and Beam Forming

3.2.1 A Novel Energy-Efficient Contention-Aware Channel Selection Algorithm for CR Networks

Agapi Mesodiakaki[1], **Ferran Adelantado**[2], **Luis Alonso**[1] **and Christos Verikoukis**[3]

[1]Technical University of Catalonia (UPC), Barcelona, Spain
e-mail: agapi.mesodiakaki@tsc.upc.edu; luisg@tsc.upc.edu
[2]Open University of Catalonia (UOC), Barcelona, Spain
e-mail: ferranadelantado@uoc.edu
[3]Telecommunications Technological Centre of Catalonia (CTTC), Barcelona, Spain
e-mail: cveri@cttc.es

In recent years, due to the ever increasing traffic demands and the limited spectrum resources, it is very likely that several cognitive radio ad hoc networks (CRAHNs) will coexist and opportunistically use the same primary user (PU) resources. In such scenarios, the ability to distinguish whether a licensed channel is occupied by a PU or by another CRAHN can significantly improve the spectrum efficiency of the network, while the contention among the CRAHNs already operating on the licensed channels with no PU activity, may further affect the performance of the network. Therefore, the proper selection of the frequency bands, already being used by other CRAHNs, could result in notable throughput and energy efficiency gains for the network under study.

To that end, in [7] we have proposed a novel energy-efficient contention-aware channel selection algorithm in a scenario where the CRAHN under study coexists with other non-cooperating CRAHNs based on a specific coexistence scheme. According to the algorithm, the CRAHN: (i) initially locates the spectrum holes by exploiting cooperative spectrum sensing (CSS) (ii) categorizes the idle licensed channels based on their contention level (i.e., number of secondary users (SUs) belonging to other non-cooperating CRAHNs that are operating on the licensed channels) and (iii) selects the less contended licensed channel to access first.

Layout: T1 Standard SC | Book ID: 318863_1_En | Book ISBN: 978-3-319-04021-9
Chapter No.: 3 | Date: 24-12-2013 | Page: 9/60

During CSS, feature detection [8, 9] is combined with a technique that estimates the number of SUs in each licensed channel. On the one hand, feature detection enables the distinction between different types of signals (e.g., PUs' and SUs' signals) at the expense of higher complexity and longer sensing time. Moreover, it requires prior information about the PU waveforms, which however, it is typically known for most standard technologies that operate on licensed channels [10]. Hence, the use of feature detection enables the distinction of the licensed channels into: (i) those with PU activity, (ii) those with SU activity and iii) those with no activity at all and it is used as the reference algorithm for the performance comparison of our approach; Please also note that the use of feature detection is fundamental, as a simpler technique (e.g., energy detection) would result in very low spectrum efficiency, as all the idle licensed channels being used by other CRAHNs, would be considered busy and thus would be avoided. On the other hand, the second technique estimates the contention in each licensed channel with SU activity. Specifically, it estimates the number of SUs belonging to the other non-cooperating CRAHNs that are already operating on the channel. Thereafter, the algorithm categorizes the idle licensed channels based on their contention level and then selects the less contended channel to be accessed first by the CRAHN under study.

In [7], it has been shown that the proposed algorithm manages to achieve notable performance gains without inducing any significant additional overhead in comparison with the reference algorithm. This is due to the fact that the performance of the algorithm only depends on the comparison between the estimated values of SUs in each licensed channel and not on their exact value. Specifically, the performance of the proposed algorithm has been evaluated by means of simulations and it has been shown that it can present gains up to 70 % in throughput and up to 68 % in energy efficiency for high traffic in the licensed channels in comparison with the reference algorithm.

In such coexistence scenarios, achieving fairness among the coexisting CRAHNs (i.e., equal transmission opportunities among their SUs) constitutes another key issue. Generally, achieving fairness among the SUs that share the same PU spectrum is a research topic that has received a lot of attention. However, most proposals assume that a licensed channel that is occupied by an SU cannot be accessed by another SU. In particular, the channel appears as being busy to the SU and thus it is avoided. To overcome the aforementioned problem, in [11], the authors propose FMAC, a MAC protocol that utilizes a three state sensing model. FMAC uses a spectrum sensing algorithm [12] to distinguish whether a busy channel is occupied by a PU or by an SU and, in the latter case, gives the option to the SU to share the channel with the SUs of other CRAHNs that are currently using it. Nevertheless, in [11] a simple system model consisting only of one licensed channel is considered, while more importantly, the scheme employs a constant back-off window. As a result, unlike the secondary network coexistence scheme (SNCS) proposed in [7], it shows low adaptability to any changes in the number of contending SUs in a licensed channel.

To that end, in [13] we evaluated the performance of SNCS in terms of fairness among the coexisting CRAHNs in comparison with FMAC by means of simulations and it has been shown that it can achieve significant throughput and energy

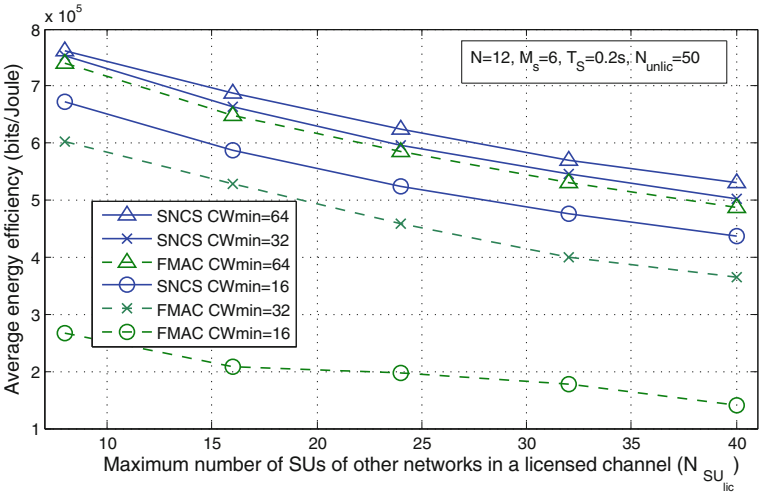

Fig. 3.3 Average energy efficiency of the CRAHN under study versus the maximum number of SUs of other networks in a licensed channel, N_{SUlic}, for different minimum back-off window values, CW_{min}

efficiency gains, while maintaining or even achieving better fairness among the coexisting CRAHNs. Please note that for the channel selection the algorithm proposed in [7] is used for both coexistence schemes.

Then, in Fig. 3.3, the average energy efficiency of the CRAHN under study is depicted for both SNCS and FMAC versus the maximum number of SUs of other networks in a licensed channel, N_{SUlic}, for different minimum back-off window values, CW_{min}.

As it can be observed, the energy efficiency of the CRAHN under study is decreased as the contention in the licensed channels increases, due to the increased number of collisions among the SUs. However, notice that the SNCS achieves better performance than FMAC for all the considered values of CW_{min}. This is due to the fact that, in FMAC, the SUs use a constant back-off window every time a collision takes place, while the SNCS employs an exponential one and thus it manages the collisions more efficiently. Therefore, the maximum performance gain of SNCS is achieved for the lowest minimum back-off window value ($CW_{\text{min}} = 16$) and for high contention in the licensed channels ($N_{\text{SUlic}} = 40$).

Moreover, as far as the fairness of the considered approaches is concerned, we employ in our study the well-known Jain's fairness index [14], which is given by:

$$J(x_1, x_2, \ldots, x_n) = \frac{\left(\sum_{i=1}^{n} x_i\right)^2}{n \sum_{i=1}^{n} x_i^2} \qquad (3.2.1)$$

where n is the number of contending SUs and x_i denotes the number of transmission opportunities of the SU i. We consider that an SU has a transmission opportunity every time it transmits a packet on the channel independently of whether a successful transmission or a collision occurs.

Layout: T1 Standard SC | Book ID: 318863_1_En | Book ISBN: 978-3-319-04021-9
Chapter No.: 3 | Date: 24-12-2013 | Page: 11/60

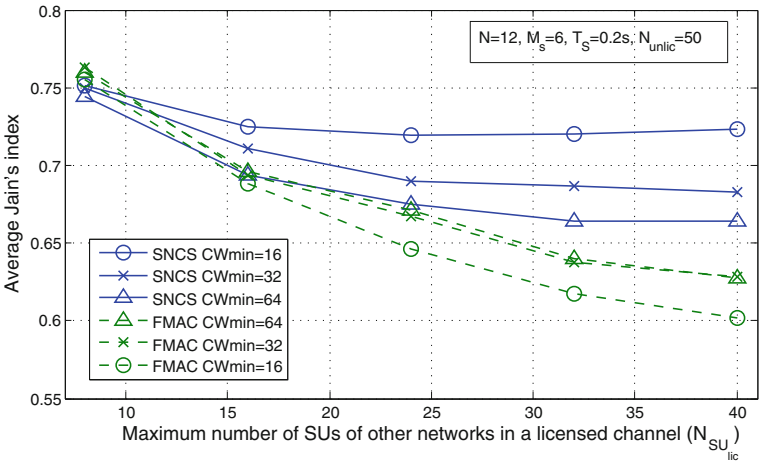

Fig. 3.4 Average Jain's index versus the maximum number of SUs of other networks in a licensed channel, N_{SUlic}, for different minimum back-off window values, CW_{min}

Then, the average Jain's index of all the SUs, that contend to gain access to a licensed channel, is depicted for both approaches in Fig. 3.4, for different minimum back-off window values, CW_{min}.

As it can be noticed, SNCS can achieve up to 25 % better fairness than FMAC ($CW_{\mathrm{min}} = 16$) for high contention in the LCs ($N_{\mathrm{SUlic}} = 40$). This stems from the fact that for short contention periods, i.e., in the case that the PU resumes its activity in the licensed channel shortly after the CRAHN under study has hopped to it, SNCS achieves much better fairness among the SUs than in FMAC, as an SU that is involved in a collision defers its transmission for a longer time, and thus the transmissions opportunities are more equally distributed among the contending SUs.

3.2.2 Cooperative CR Beam Forming in the Presence of Location Errors

Auon Muhammad Akhtar[1], **Luca De Nardis**[2], **Mohammad Reza Nakhai**[1], **Oliver Holland**[1], **Maria Gabriella Di Benedetto**[2] **and A. Hamid Aghvami**[1]

[1]King's College London, London, UK
e-mail: auon.akhtar@kcl.ac.uk; reza.nakhai@kcl.ac.uk; oliver.holland@kcl.ac.uk
[2]Sapienza University of Rome, Rome, Italy
e-mail: lucadn@newyork.ing.uniroma1.it; dibenedetto@newyork.ing.uniroma1.it

3.2.2.1 Background and Purpose

Thus far, most of the research on cognitive radio has been focused on single-hop scenarios, tackling physical (PHY) layer and/or medium access control (MAC) layer issues. However, recent research finding have highlighted the potentials of multi-hop cognitive radio networks [15]. The cognitive paradigm can be applied to different scenarios of multi-hop wireless networks, one such scenario being the cognitive radio ad hoc network which consists of CR nodes which communicate with each other in a peer to peer fashion through ad hoc connections [16]. To fully realize the potential of such networks, cross-layer design issues must be addressed, for example, the routing decisions at the network layer should be made in conjunction with the PHY layer characteristics.

This chapter, summarising work first presented in [17], introduces a transmit beamforming strategy taking into account the positions of primary, secondary victim and intended secondary receivers, to achieve underlay secondary access in multihop cognitive radio networking. The transmit beamforming strategy defines a novel path optimization scheme that deviates from a preselected path given by the routing module, based on local information and according to a relay selection metric. This metric is designed to improve both coexistence with primary/secondary victim receivers and performance of the secondary cognitive network. Simulations compare the proposed strategy with a baseline solution that does not adopt beamforming, and with a strategy that applies beamforming on each hop without modifying the original path. Results show that the proposed strategy is capable of improving coexistence with primary/secondary victims, and highlight that a trade-off exists between the meeting of coexistence constraints and maximisation of secondary network performance.

3.2.2.2 Transmit Beamforming Strategy

A first key element of this work is the transmit beamforming strategy between hops in the path. This strategy aims to minimize the total transmitted power subject to certain constraints. These constraints are the interference margins of the primary nodes and minimum signal-to-noise ratio/signal-to-interference-and-noise ratio (SNR/SINR) requirements of the secondary nodes. Instead of using instantaneous channel state information (CSI), we use the second order statistics of the channel state information at the transmitting nodes. It is assumed that the secondary transmitters have knowledge about the locations of all the primary nodes within their transmission range. Instead of using a large number of samples to obtain the second-order statistics, we use the expression derived in [18] to obtain these statistics directly. Based on this, an optimisation problem is derived to minimise the transmit power at the beamforming secondary node, subject to constraint of a minimum required SINR at the secondary receiver and an interference threshold at all primary receivers [17]. Since the resulting problem is non-convex, it is

Layout: T1 Standard SC | Book ID: 318863_1_En | Book ISBN: 978-3-319-04021-9
Chapter No.: 3 | Date: 24-12-2013 | Page: 13/60

converted into convex sequential dynamic programming (SDP) form, which can solved by an SDP solver like SeDuMi. More information on the procedure for this is available in [17].

3.2.2.3 Routing Algorithm Design

We next utilize transmit beamforming to design a routing algorithm for multi-hop cognitive radio networks. The objective of the algorithm is three-fold: (i) To minimize the end to end power consumption, (ii) To minimize the co-channel interference generated within the secondary network, and (iii) To minimize the number of primary interference constraint violations.

To achieve the goals set above, we adopt a centralized approach whereby the optimal power saving route is initially calculated through Dijkstra's algorithm by using the point to point link costs without beamforming. After this initial step, the algorithm modifies the selected route by using a novel cost metric. To ensure that the modified route does not deviate too much from the optimal power saving route, the cost metric is used only on alternate hops, for example, for every odd numbered hop of the optimal route, the hop destination is selected based on the proposed cost metric, while the destinations of the even numbered hops remain unchanged.

We now propose a cost metric which is used to select the node which is most suitable to act as a relay. The proposed metric takes into account the potential impact of the selection of a relay on the primary receivers and other secondary nodes, within the transmission range of the source and the candidate relay node. In the following, we refer to the source, relay and destination nodes as S, R and D, respectively. A terminal R will only be eligible as a relay if it meets all the following conditions:

(1) S does not violate the interference constraint of any of the primary users when it transmits data to R using beamforming;
(2) R does not violate the interference constraint of any of the primary users when it transmits data to D using beamforming;
(3) The position of R is such that the distance between R and D, indicated as $dist_{RD}$, is not larger than the distance from S to D, $dist_{SD}$. This condition ensures physical connectivity between the selected relay and D and it ensures that the algorithm remains loop free. The above description translates into the cost $Cost(S,D,R)$ associated to the generic terminal R as a potential relay between S and D.

Further information on the associated cost function can be obtained in [17]. However, for the purpose of this chapter, Fig. 3.5 gives a demonstration of the proposed cost metric in action. Here, green nodes are the secondary source and destination nodes, the yellow nodes are the primary nodes while the nodes labelled as *R1*,…,*R6* are the candidate relay nodes. Amongst the candidate relay nodes, the nodes in blue are the eligible candidates while the nodes in red, i.e., *R4* and *R6* are

Layout: T1 Standard SC | Book ID: 318863_1_En | Book ISBN: 978-3-319-04021-9
Chapter No.: 3 | Date: 24-12-2013 | Page: 14/60

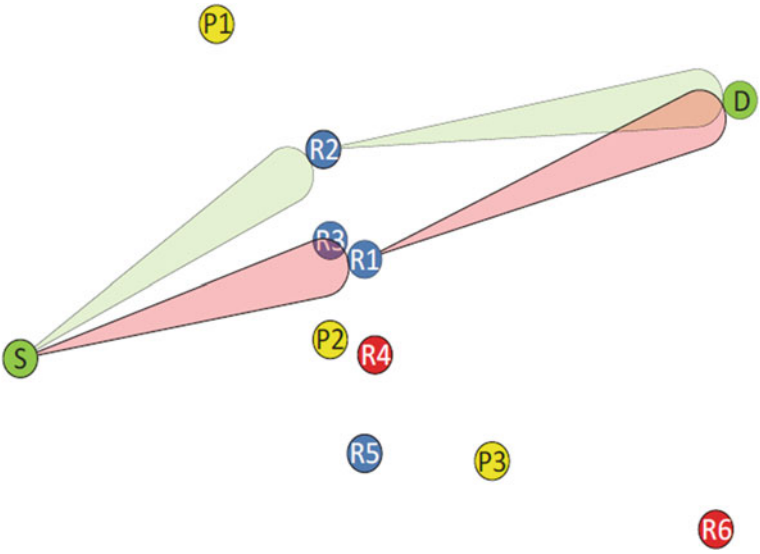

Fig. 3.5 Demonstration of the proposed cost metric

not eligible to act as relays. *R4* is rejected because *S* cannot transmit to *R4* without violating the interference constraint of *P2* while the distance between *S* and *R6* is larger than the distance between *S* and *D*. The Dijkstra's algorithm selects *R1* as the best option to act as a relay. However, it can be seen that if the data is transmitted to *R1*, a lot of interference is exerted upon *R3*. On the other hand, if *R3* is selected as relay, interference will be exerted upon *R1* when *R3* forwards the data to *D*. Using the proposed cost metric, the best option here is to select *R2* as relay.

3.2.2.4 Performance Evaluation

The performance of the proposed solution is evaluated by means of computer simulations executed by combining MATLAB and OMNeT++ as follows:

(1) MATLAB was used to implement the transmit beamforming strategy introduced in Section III and to analyse the performance of the route optimization approach defined in Section IV by measuring the interference generated towards each secondary node as well as the average number of constraints set by primary receivers that are met.
(2) OMNeT++ was used to test the proposed strategy in presence of actual packet transmissions in order to measure the impact of the proposed solution on throughput, moving from results generated in MATLAB.

Layout: T1 Standard SC | Book ID: 318863_1_En | Book ISBN: 978-3-319-04021-9
Chapter No.: 3 | Date: 24-12-2013 | Page: 15/60

3.2.2.5 Simulation Scenario and Setup

The MATLAB code was used to simulate a network of secondary nodes equipped with a ULA with $N = 8$ antenna elements and a spacing between adjacent elements $d = 0.0625$ m, corresponding to half a wavelength for a carrier frequency $f_c = 2.4$ GHz, and capable thus to perform DOA estimation and beamforming. An angular spread $\Delta\theta = 2^o$ was introduced around the exact angle for each measurement. A noise power $P_n = -101$ dBm was assumed at each receiver, while the path loss exponent for propagation was set equal to $\alpha = 2$. MATLAB was used to solve the beamforming optimization problem of taking advantage of the SeDuMi solver provided by the cvx package, imposing an upper bound φ_m on the allowed interference towards the primary nodes and a minimum SNR level of $\gamma_r = 10$ dB for all the secondary nodes.

The following steps were executed in MATLAB for each run:

(1) Generation of a topology composed of N_S secondary nodes and N_P primary nodes randomly deployed in an area of $X_{max} = 50$ m by $Y_{max} = 50$ m^2;
(2) Generation of N_{conn} connection requests in the secondary network with random source and destination nodes, random duration uniformly distributed between *minDuration* and *maxDuration* and random delay from the previous connection request from same source node uniformly distributed between *minDelay* and *maxDelay*; then, for each connection request: (a) Selection of the best path according to the minimum power routing strategy defined previously in this chapter; (b) Optimization of the path according to the proposed metric, described previously and in detail in [17]; (c) Measurement of interference generated towards secondary nodes not involved in the connection with and without optimization; (d) Measurement of number of primaries for which the constraint on the maximum interference value is met with and without optimization.
(3) Export to file of the data required by OMNeT++, consisting of: (a) primary and secondary network topology; (b) the list of the N_{conn} generated connection requests, including source, destination and duration; (c) original and optimized paths for each connection; (d) the reduction in the interference $I(x, y, z)$ perceived in y guaranteed by the introduction of beamforming in the link from x to z, for all x–z pairs involved in any connection, for both original and optimized paths.

The inputs generated in MATLAB were used in a simulated secondary network built in OMNeT++, with each secondary node characterized by the architecture shown in Fig. 3.6. With reference to such architecture, it should be noted that:

- The mobility and clustering modules were not activated, as a static network with flat organization was assumed.
- The positioning module was configured so to provide perfect position information about all network nodes.
- The application module for a generic node x was in charge of reading from file connection requests having x as source, and generate for each connection

Layout: T1 Standard SC | Book ID: 318863_1_En | Book ISBN: 978-3-319-04021-9
Chapter No.: 3 | Date: 24-12-2013 | Page: 16/60

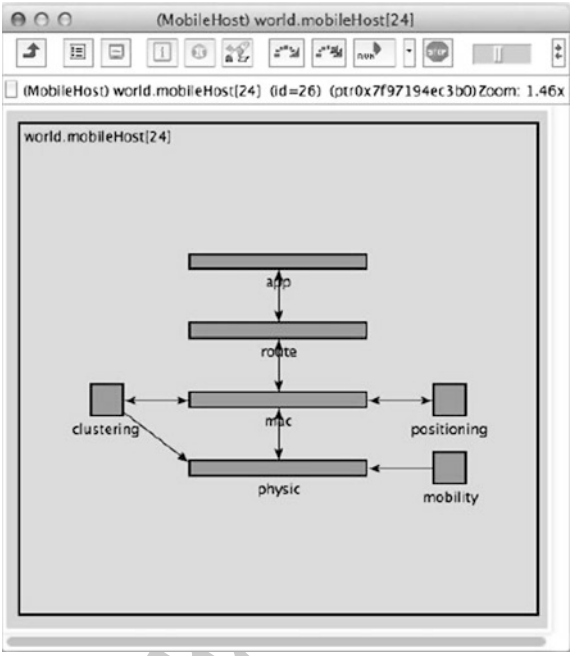

Fig. 3.6 Secondary node architecture implemented in OMNeT++

packets of size *appPacketSize* bits spaced in time by a constant delay set to *applicationRate*/*appPacketSize* (modeling thus a Constant Bit Rate (CBR) packet stream) for a time equal to the connection duration read from file;

- The routing module for a source node x, upon receiving from the application module the first packet of a connection, was in charge of (a) loading from file the corresponding end-to-end path determined in MATLAB, (b) record such path in each packet; the routing module of intermediate nodes took care of forwarding the packet towards the destination by reading the next hop from the packet itself, while routing module of a destination node simply forwarded the packet to application module.
- The MAC module implemented a simple Aloha protocol without retransmission, taking care of immediately forwarding packets received from the routing module to the physical layer module and vice versa.
- The physical layer module had the responsibility of transmitting and receiving packets taking into account path loss, propagation delays and interference generated by packet collisions.

The impact of interference, in particular, was modelled with accuracy significantly higher than what currently found in existing OMNeT++ frameworks, such as INET and MixiM, in order to ensure a correct analysis of the impact of the proposed optimization on network performance. The simulator is in fact able to

keep track of all transmitted packets and, for each packet reception, determines the interference level on a symbol by symbol basis (note that, as binary modulation was considered in all simulations, in the following bits will be considered in place of symbols). Consecutive bits subject to the same interference are grouped into so called bit regions. Next, for each bit region the average Bit Error Probability (BEP) is evaluated by adopting the Standard Gaussian Approximation for the interference power, and the number of bit errors is randomly determined according to the BEP. Finally, the total number of bit errors generated is evaluated by summing up errors introduced in each bit region, and compared with the maximum number of errors admitted for the packet as determined by the adoption of a Reed-Solomon code with a coding rate $RS_{\text{rate}} = 0.835$ (corresponding to a correction capability roughly equal to 10 % of the packet bits) in order to decide if the packet is correctly received or discarded. The following steps were executed in OMNeT++ for each run: (1) Loading of primary and secondary network topologies from file; (2) Loading of connection requests from file and for each request: (a) Generation of packets; (b) Forwarding of packets along the end-to-end path read from file; (c) Measurement of end-to-end throughput and other relevant metrics; (3) Averaging of measured metrics.

Table 3.1 presents the values for the simulation parameters.

3.2.2.6 Simulation Results: Matlab

(1) Figure 3.7 shows the average interference imposed on the secondary nodes when the data is routed between the secondary source and destination nodes. To ensure continuity of the simulations, the constraint on primary interference is relaxed if the cost of is $+\infty$ for all the secondary nodes within the transmission range of the transmitter for a specific hop. As can be seen from the figure, the optimized routing with beamforming, i.e., routing with the proposed cost metric, gives the best performance in terms of interference imposed within the secondary network. As expected, routing without beamforming gives the worst performance. Furthermore, it must be mentioned here that to compare the performance of routing with beamforming and optimized routing with beamforming, one must also consider the number of primary constraint violations, since we relax the primary interference constraint when none of the secondaries is able to satisfy this constraint. To make this comparison, Fig. 3.8 shows the number of primary constraint violations for different number of primary nodes. From Figs. 3.7 and 3.8, it can be seen that the difference in performance between the optimized and non-optimized routing with beamforming in Fig. 3.7 is large when the corresponding difference in primary violations in Fig. 3.8 is relatively small, e.g., the performance when the number of primary nodes is 30. Otherwise, when the difference in performance in Fig. 3.7 is small, the difference in the number of primary constraint violations is relatively large. In order to have a fair comparison between the two, the number of

Layout: T1 Standard SC | Book ID: 318863_1_En | Book ISBN: 978-3-319-04021-9
Chapter No.: 3 | Date: 24-12-2013 | Page: 18/60

Table 3.1 Simulation parameters

Parameter	Value(s)
Number of Secondary nodes N_S	50
Number of primary nodes N_P	From 10 to 50
Number of connection requests per run N_{conn}	1000
Minimum connection duration *minDuration*	25 s
Maximum connection duration *maxDuration*	75 s
Min delay between connection requests *minDelay*	50 s (High Traffic)/500 s (Low Traffic)
Max delay between connection requests *maxDelay*	100 s (High Traffic)/750 s (Low Traffic)
Transmission rate at physical layer	1 Mb/s
Maximum transmission power for secondary nodes	1 μW
Application packet length *appPacketSize*	512 bits
Application source rate *applicationRate*	320 kbit/s

primary constraint violations for routing with beamforming and optimized routing with beamforming should force to be the same.

3.2.2.7 Simulation Results: OMNeT++

OMNeT++ simulations considered the following four different scenarios, obtained by varying the traffic load in the secondary network and the number of primary nodes:

- *Low traffic, free network*—Low traffic (obtained by setting the *minDelay* and *maxDelay* variables to the corresponding values in Table 3.1) and no primary nodes;
- *Low traffic, constrained network*—Low traffic and $N_P = 10$ primary nodes;
- *High traffic, free network*—High traffic (obtained by setting the *minDelay* and *maxDelay* variables to the corresponding values in Table 3.1 and no primary nodes;
- *High traffic, constrained network*—High traffic and $N_P = 10$ primary nodes.

The throughput, defined as the ratio between end-to-end received packets and generated packets was measured in the four scenarios above for the three strategies previously introduced in the paper. Figure 3.9a presents the throughput in the case of the Low traffic, free network scenario. The figure shows that in this scenario the optimization in the routing path leads to an increase in throughput, as on each other hop the strategy is able to select the node that provides the lowest amount of interference to neighbouring nodes, thus increasing the probability of correct packet reception throughout the network. Moving to the Low traffic, constrained network scenario, Fig. 3.9b shows that the introduction of constraints determined by the presence of a significant number of primaries has the impact of reducing the gap between the two BF-based strategies, due to the fact that in several cases potential relays that would lead to lower interference in the secondary network are

Layout: T1 Standard SC | Book ID: 318863_1_En | Book ISBN: 978-3-319-04021-9
Chapter No.: 3 | Date: 24-12-2013 | Page: 19/60

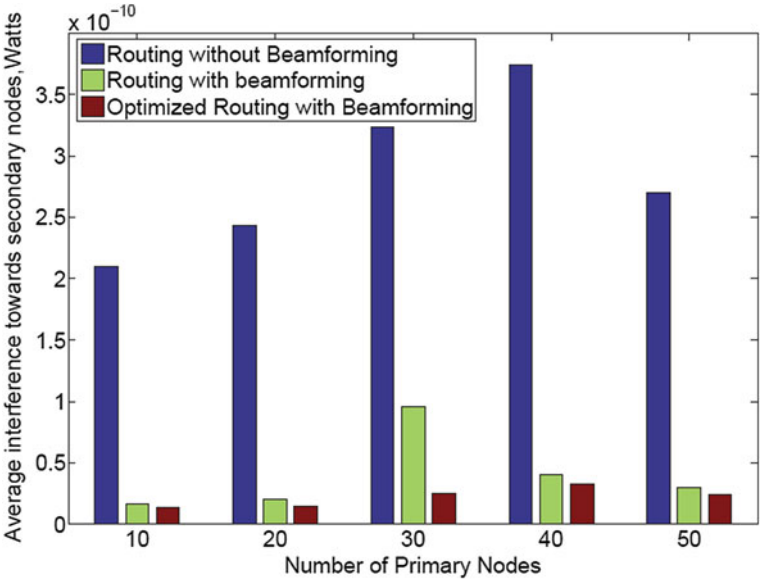

Fig. 3.7 Average total interference exerted upon the secondary nodes between source and destination

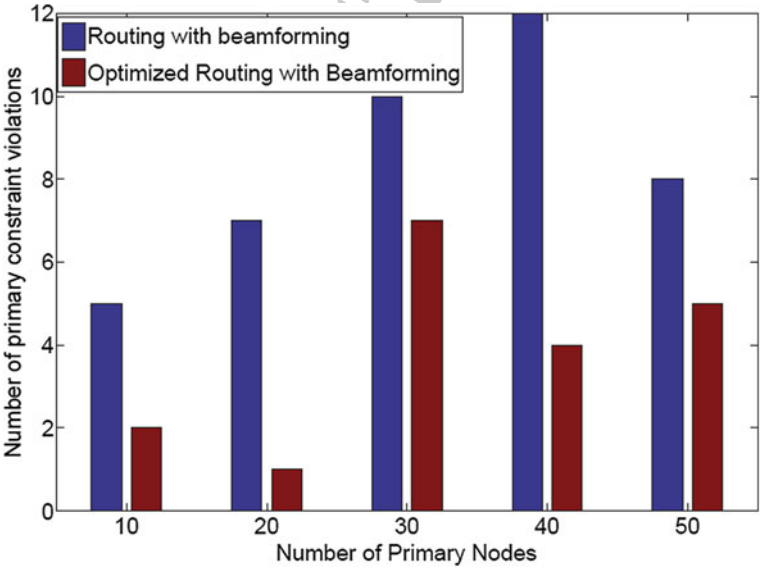

Fig. 3.8 Number of primary constraint violations

Layout: T1 Standard SC | Book ID: 318863_1_En | Book ISBN: 978-3-319-04021-9
Chapter No.: 3 | Date: 24-12-2013 | Page: 20/60

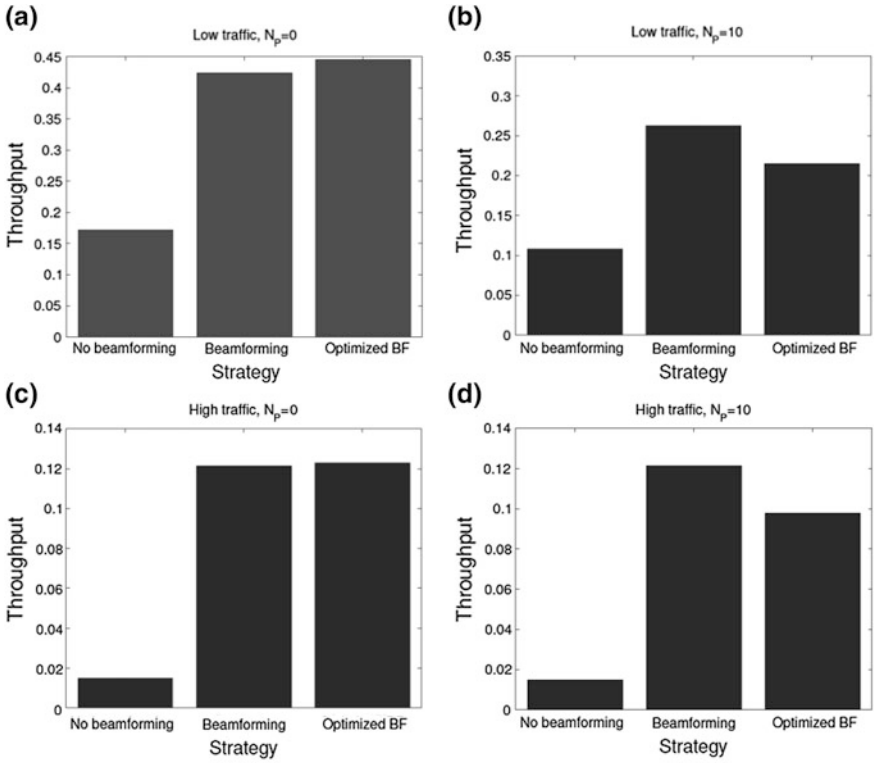

Fig. 3.9 Number of primary constraint violations. **a** Throughput in the Low traffic, free network scenario for the three considered routing strategies **b** Throughput in the Low traffic, constrained network scenario for the three considered routing strategies **c** Throughput in the High traffic, free network scenario for the three considered routing strategies **d** Throughput in the High traffic, constrained network scenario for the three considered routing strategies

discarded as they do not satisfy the hard constraint on the level of interference towards one or more primary receivers. Figure 3.9c shows how the throughput is affected in the High traffic, free network; results show how for all strategies performance is significantly reduced due to the higher number of collisions, and the corresponding higher average value of the interference power during packet reception. Finally, Fig. 3.9d shows results in the High traffic, constrained network, that introduces again the presence of the primary nodes; interestingly, results highlight that in this case the Optimized Routing with Beamforming leads to slightly worse results compared to simple Routing with Beamforming. However, as shown by Fig. 3.8, this comes together with a better coexistence capability with primary receivers, highlighting the presence of a trade-off between coexistence and secondary network performance.

3.2.2.8 Conclusions

This chapter has focused on transmit beamforming and routing in a multihop, ad hoc cognitive radio network. After introducing the transmit beamforming strategy, we proposed a new cost metric which was used to design an optimized, beamforming based routing algorithm with three-fold objective: to minimize the end-to-end path power consumption; to minimize the co-channel interference imposed within the secondary network and to minimize the number of primary interference constraint violations. Simulation results from MATLAB have confirmed that the optimized routing algorithm outperformed the original routing algorithm in terms of both, the interference generated within the secondary network and the number of primary interference constraint violations. The simulations carried out in OMNeT++ confirmed the improved throughput of the secondary network when no constraints from primary nodes are imposed, while they highlight a trade-of between coexistence capability and secondary network performance when the presence of primary nodes is taken into account.

Acknowledgements This work has been supported by the ICT-ACROPOLIS Network of Excellence, FP7 project no. 257626, www.ict-acropolis.eu, COST Action IC0902, and the UK's Mobile VCE Consortium.

3.3 Spectrum Aggregation over Non-contiguous Frequency Bands

Filippo Meucci[1], **Orlando Cabral**[1], **Fernando J. Velez**[1], **Jessica Acevedo Flores**[1], **Daniel Robalo**[1], **Albena Mihovska**[2], **Neeli R. Prasad**[2] **and Oliver Holland**[3]

[1]UBI-Instituto de Telecomunicações, Aveiro, Portuga
[2]University of Aalborg, Aalborg, Denmark
[3]King's College London, London, UK

Dynamic spectrum access (DSA) techniques are promising to enable spectrum aggregation with intra-operator multi-band scheduling [19]; hence, alleviating the spectrum scarcity problem.

Spectrum Aggregation (SA) consists in aggregating several (and possibly) fragmented bands, exploiting multiple small spectrum fragments simultaneously to yield to a (virtual) single larger band and ultimately deliver a wider band service. Consequently, SA allows that new high data rate wireless communication systems can coexist while reusing the spectrum of legacy systems. The non-contiguous approach may provide larger flexibility as well as diversity.

Layout: T1 Standard SC | Book ID: 318863_1_En | Book ISBN: 978-3-319-04021-9
Chapter No.: 3 | Date: 24-12-2013 | Page: 22/60

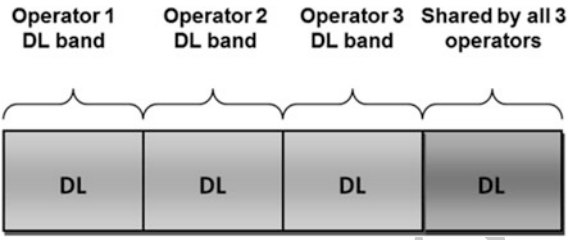

Fig. 3.10 Scenario of common frequency pool

3.3.1 Spectrum Aggregation with Multi-band User Allocation Over Two Frequency Bands

Affordable, high-bandwidth mobile access improves the quality of experience for users, enabling them to get more out of existing services and opens up opportunities for new mobile broadband services. Supporting additional system capacity and higher data rates will improve the value of these services. However, this is impeded by the existing highly fragmented radio frequency spectrum that does not match the actual demand for transmission and network resources. Therefore, mobile operators might be forced to aggregate spectrum of two or more separated sub-bands for downlink (DL) and uplink (UL) bands.

3.3.1.1 Problem Statement

The objective is to determine the best user allocation for a single operator over two (or more) High Speed Downlink Packet Access (HSDPA) frequency bands in order to maximize the total network throughput. The operator has exclusive usage of the 2 GHz band and can access the shared frequency pool at 5 GHz. The quantity of radio resources available at 5 GHz is determined by spectrum trading (or bargaining) among all the operators that have been granted access to the frequency pool, as shown in Fig. 3.10.

The problem of scheduling the users into two bands can be formulated as an Integer Programming optimization problem [20, 21]. The total throughput of the operator is the profit function to be maximized. The profit function depends on the channel qualities and on the number of users in each band. The number of users that can be allocated in the primary band (i.e., 2 GHz) are determined based on the load thresholds; then the multi-band scheduling is determined as a General Assignment Problem (GAP) [20] where the number of users in each band is upper bounded.

3.3.1.2 General Multi-band Scheduling: Spectrum Sharing as a General Assignment Problem

Profit Function. Solving Multiple-Objectives GAP (MO-GAP) can be very difficult and usually the objectives are combined together via a linear combination, called "scalarization" [20].

The profit function (PF) for the maximum throughput in the GMBS is the following:

$$(\mathrm{PF}) \quad \max \sum_{b=1}^{m} \sum_{u=1}^{n} R_{bu} x_{bu} \tag{3.3.1}$$

where R_{bu} is the throughput for user u on band b and x_{bu} is a 0–1 integer variable $x_{bu} \in \{0, 1\}$ defining the user allocation over the bands that is mathematically represented by:

$$x_{bu} = \begin{cases} 1 \text{ if user u is allocated on band b} \\ 0 \text{ otherwise} \end{cases}$$

For a single transceiver User Terminals (UTs), the GMBS has two constraints:

1. Each user can be allocated only to a single frequency band (assumption of single transceiver UT), which is represent by the integrality of $x_{bu} \in \{0, 1\}$;

The total number of users on each band is upper bounded; this is the bandwidth constrain (BC) on each frequency band, which is reported in Eq. 3.3.2.

$$\sum_{u=1}^{n} x_{bu} \leq N_b^{max} \; for \; b = 1 \ldots m \tag{3.3.2}$$

In general, the throughput R_{bu} is a function of the channel quality of user u on band b, $R_{bu} = f(CQI_{bu})$, where CQI_{bu} is dependent on the Signal to Interference Ratio (SIR) that depends on the propagation conditions, on the interference from other cells and on power per code available:

$$CQI_{bu} = f(SIR) \tag{3.3.3}$$

The higher the number of users allocated in the band, the lower the CQI. *Rbu* can be changed ahead to depend on other variables, however, for simplicity in this work, it is dependent only on the CQI.

$R_{bu} - x_{bu}$ *interrelation: two step GMBS procedure*. The General Multi-Band Scheduling (GMBS) aims to determine $x_{bu} \forall u = 1 \ldots n \; ; \quad \forall b = 1 \ldots m)$ or the allocation of the users over the available frequency bands in order to maximize the total throughput. As such, the interdependence of R_{bu} with x_{bu} needs to be solved. AQ4

Layout: T1 Standard SC | Book ID: 318863_1_En | Book ISBN: 978-3-319-04021-9
Chapter No.: 3 | Date: 24-12-2013 | Page: 24/60

The GMBS problem is formulated in two steps. First, the maximum number of users that can be allocated on each frequency band is determined, then R_{bu} is defined as the available throughput considering that N_{max} users are allocated in the band. The number of maximum users in each band is calculated depending on the load, as $N_b^{max} = L_{normalized}^{-1}$, where $L_{normalized}$ is estimated based on the resources available for the cell, estimated as follows:

$$L_{normalized}(i) = \frac{\sum_{u=1}^{N_b} Load(u)}{R_{HSDPA}} \tag{3.3.4}$$

where: N_b is the number of HSDPA user in band b, R_{HSDPA} is the number of High Speed Downlink Shared Channel (HS-DSCH) allocated in the cell, and $Load(u)$ is the average number of HS-DSCH required by user u to support its service rate, $R(u)$. This number is given by the following Eq. 3.3.5:

$$Load(u) = \frac{R(u)}{R(CQI_{bu}) \bullet N_{HS-PDSCH}(CQI_{bu})} \tag{3.3.5}$$

where: the average propagation condition determines the channel quality indicator ID of user u on band b, CQI_{bu}, $R(CQI_{bu})$ is the achieved bit rate when one CQI_{bu} block is allocated in every frame and $N_{HS\text{-}PDSCH}(CQI_{bu})$ is the number of HS-DSCH associated to CQI_{bu}.

Once N_b^{max} has been determined, R_{bu}, or the expected data rate for each user should be dependent on CQI_{bu}, the effective packet error rate (PER) experienced (or predicted based on the position in case of a first transmission), and the number of users:

$$R_{bu} = \frac{R(CQI_{bu})}{N_b} \times (PER_{bu})^{-1} \tag{3.3.6}$$

The direct mapping between CQI_{bu} and the throughput can be expressed as:

$$R(CQI_{bu}) = \begin{cases} 188.5 \text{ if } CQI_{bu} = 5 \\ 396.0 \text{ if } CQI_{bu} = 8 \\ 1659.5 \text{ if } CQI_{bu} = 15 \\ 3584 \text{ if } CQI_{bu} = 22 \end{cases} \tag{3.3.7}$$

Suboptimal Multi-Band Allocation Algorithm. UTs are able to use both of the frequencies. The Common Radio Resource Management (CRRM) entity keeps track of the CQI in both frequencies by making use of the pilot channel. By keeping the load at the same level, users may be scheduled on one frequency or another, depending also on the CQI available. When a user arrives to the system, the UT is allocated to the 2 GHz band. The load is checked in both bands. If the load is higher in the 2 GHz, the user with the highest CQI in the 2 GHz will be moved to the 5 GHz band. The load is estimated based on the resources available for the cell. The procedure is the same as proposed in [22].

Layout: T1 Standard SC | Book ID: 318863_1_En | Book ISBN: 978-3-319-04021-9
Chapter No.: 3 | Date: 24-12-2013 | Page: 25/60

Results. The performance of the algorithm is assessed by using the service throughput which is the total number of bits transmitted and correctly received by the all users in the cell:

$$Serv\_thr_{[s^{-1}]} = \frac{b_{serv}[p]}{k \cdot T} \tag{3.3.8}$$

where: $b_{serv}[p]$ is the number of bits received in given period p, T is the transmit time interval, k is the number of steps. $k \cdot T$ is the simulation duration. Users are displaced in the cell within a distance from the BS from 300 to 3000 km with uniform distribution. The Near Real Time Video (NRTV) calls are modeled by a Poisson distribution, the call duration is exponentially distributed with an average of 180 s.

Figure 3.11a shows the results without multi-band scheduling (MBS). The operator has the availability of two frequency bands and each one is managed separately; calls requests are divided in the two bands and it is not possible to switch a service from one band to the other. The "*Overall Serv*" is the sum of the service throughput in both bands, the traffic requirement is the traffic required to satisfy all the users.

Figure 3.11b shows the results with the MBS, the operator can decide on which band to allocate the user. It is shown that, even for a single-band UT, both bands have a higher throughput due to the switching of users between them. Figure 3.12 compares the results with and without MBS. A 200 Kbps improvement is evident over a wide range of UTs in the cell.

By use of MBS a constant throughput gain over a wide range of active services in the cell can be achieved. MBS is able to support a higher number of NRTV users due to the ability of scheduling users considering their respective radio channel quality in different parts of the radio spectrum. The achieved improvement is relative to a scenario where users are randomly displaced in the cell. Because the 5 GHz bandwidth has much lower coverage then the 2 GHz band, the results shown here are a first step towards the analysis of the attainable gain.

3.3.2 Integrated Common Radio Resource Management with Spectrum Aggregation

Radio Resource Management (RRM) plays an important role in wireless system design, due to the scheduling algorithm which decides among packets that are ready for transmission, allowing certain quality of service (QoS) levels be achieved. Common RRM (CRRM) refers to the set of functions that are devoted to ensure an efficient and coordinated use of the available radio resources in heterogeneous networks scenarios, as shown in Fig. 3.13.

A non-contiguous SA (from an upper layer point of view) and an integrated CRRM (iCRRM) entity are proposed, where SA and CRRM functionalities are handled simultaneously. The proposed iCRRM enables the integration of spectrum and network resource management functionalities leading to higher performance and system

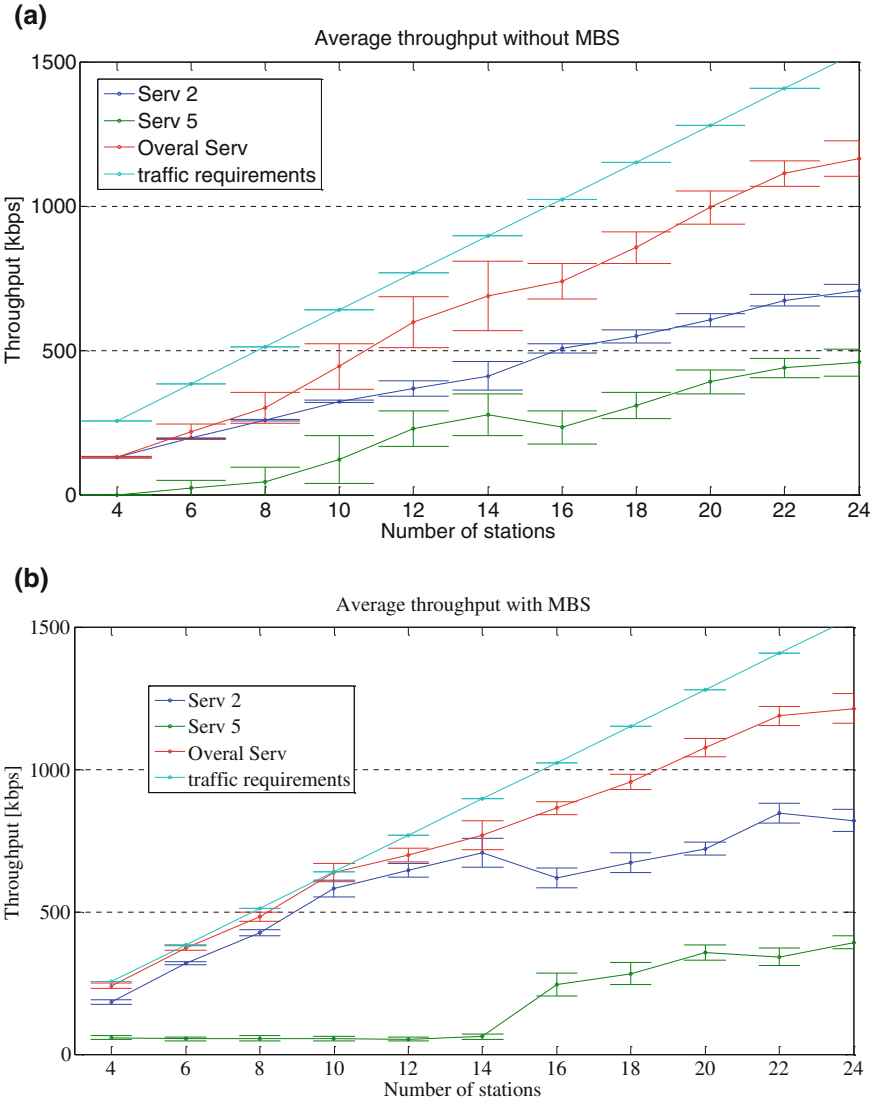

Fig. 3.11 Average throughputs: **a** without MBS, **b** with MBS

capacity gains, performing the scheduling via the optimal solution of a GMBS problem. The integration of dynamic spectrum use and SA, achieved with the use of iCRRM techniques is shown to provide significant throughput gain compared to a system where the iCRRM is not used. A formulation is proposed for the average Signal to Interference-plus Noise Ratio (SINR) that allows for setting the basic limits for the dependence of SA with GMBS on the coverage distance with an optimal solution. This

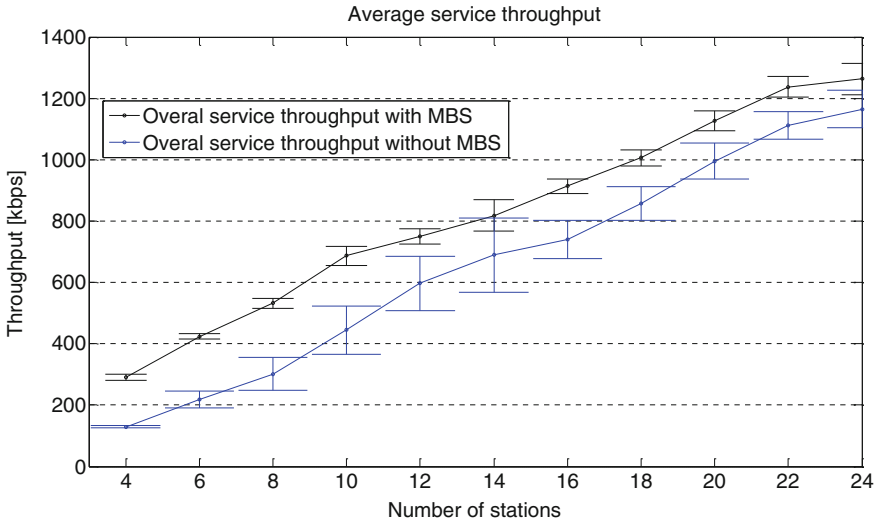

Fig. 3.12 Service throughput with and without MBS

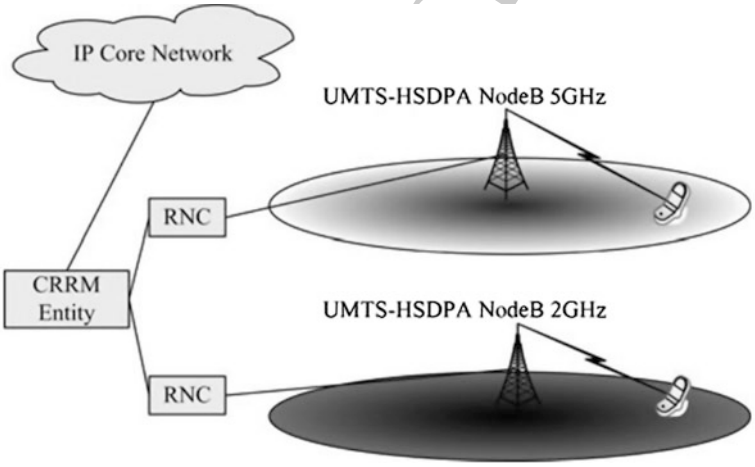

Fig. 3.13 CRRM in the context of SA with two separated frequency bands

section addresses radio resource management with spectrum aggregation. It discusses innovative results for communications using multiple bands to improve overall throughput and reduce packet delay for future mobile communication systems.

Table 3.2 Parameters and models used for 2 GHz and 5 GHz bands

Carrier frequency	2 GHz	5 GHz
Bandwidth BW	5 MHz	5 MHz
Path loss model	$L_{2GHz} = 128.1 + 37.6 \cdot \log_{10}(R)$	$L_{5GHz} = 141.5 + 28 \cdot \log_{10}(R)$

3.3.2.1 Objective and System Model

The inclusion of the iCRRM in the system model is used to facilitate the best user allocation and maximize the total network throughput in HSDPA systems, considering two frequency bands b are considered 2 GHz and 5 GHz with frequency reuse pattern one.

The radio channel follows the ITU radio propagation models, as summarised in Table 3.2. The interference in the Mobile Station (MS) is calculated with the signal strength received from the first ring of neighboring Base Stations (BSs) and the thermal noise [23].

Considering u as the user index, the CQI is a mapping of the averages of the CQIs recorded over time; a direct mapping between CQI_{bu} and the available rate at the physical layer, in kbps, is shown in "$R_{bu} - x_{bu}$ interrelation: two step GMBS procedure".

3.3.2.2 General Multi-band Scheduling

The Profit Function (PF) maximizes the total throughput of the operator, and is defined considering the ratio between the rate available on the single DL channel and the requested rate by the service flow and is expressed as follows:

$$(PF) \sum_{b=1}^{m} \sum_{u=1}^{n} W_{bu} x_{bu} \tag{3.3.9}$$

where: x_{bu} is the allocation variable, n the number of users and the normalized metric W_{bu} is:

$$W_{bu} = \frac{[1 - PER(CQI_{bu})] \cdot R(CQI_{bu})}{S_{rate}} \tag{3.3.10}$$

where: S_{rate} is the NRTV service rate, $PER(CQI_{bu})$ is the average Packet Error Rate (PER) occurred in previous transmissions that the DL channel for user u on band b is suffering for the Modulation and Coding Scheme (MCS) supported (0 in the case no transmissions has ever occurred), and $R(CQI_{bu})$ is the DL channel throughput for user u on band b, as a function of the MCS supported.

The constraints for GMBS vary, depending on the ability of the MSs to simultaneously transmit and receive in multiple frequencies (multiple transceivers at the MS), or just over a single band at the time. HSDPA physical layer [24] provides a set of orthogonal codes available for data transmission within a

sub-frame. Codes maybe allocated to service flows/users in a flexible manner. More than one code can be assigned to a single user or a single code can be assigned to more than one user. The users on the same code adopt a time-division multiple access which is managed by the packet scheduler. The allocation variable x_{bu} reflects the code allocation per users and is either a Boolean value in the case of single code allocation, or a positive integer, $x_{bu} \in \{0, 1, \ldots, \max(N_{codes})\}$, in the case of multi-code allocation.

In the following explanation, a single-frequency single-code allocation will be explored with a Round Robin (RR) scheduler. The RR scheduler was selected since it is the one with least interference on upper layer algorithms.

In single-frequency single-code allocation, the GMBS presents the following constraints:

1. Allocation Constraint (AC): each user can be allocated only to a single frequency band with a single orthogonal code:

2. $$(AC) \sum_{b=1}^{m} x_{bu} \leq 1, x_{bu} \in \{0, 1\}, \forall \text{ user } u \tag{3.3.11}$$

3. Bandwidth Constraint (BC): the total number of users on each band is upper bounded by the maximum normalised load that can be handled in the band, $L_b^{max} \in [0, 1]$:

4. $$(BC) \sum_{b=1}^{m} \frac{S_{rate} \cdot (1 + R_{Tx} \cdot PER(CQI_{bu}))}{N_{codes} \cdot R(CQI_{bu})} \cdot x_{bu} \leq L_b^{max}, \forall \text{ b and } b \tag{3.3.12}$$

where: the first term is the requested serviced at a rate for user u, including the packet loss, normalized with the maximum data rate that the network can offer to the user u on band b which is $N_{codes} \cdot R(CQI_{bu})$ where N_{codes} is the maximum number of parallel codes available in HSDPA. $R_{Tx} = 2$ is the number of H-ARQ retransmissions. BC accounts for the user traffic requirement, DL capacity and overhead caused by packets lost. The load constraint for each band, L_b^{max}, is lower than one because of the padding caused when the packets from upper layers are fragmented to fit the MAC Packet Data Unit (MPDU), and signaling overhead.

3.3.2.3 Average SINR Analysis with Unitary Frequency Reuse Pattern

The SA gain is going to be evaluated for several inter-cell distances with a frequency reuse pattern K, equal to one. The average SINR was obtained following a similar method to the one described in [25]. In order to have comparable results, SA needs to be analyzed at constant average SINR, which is achieved only by tuning the BSs transmitter power.

Layout: T1 Standard SC | Book ID: 318863_1_En | Book ISBN: 978-3-319-04021-9
Chapter No.: 3 | Date: 24-12-2013 | Page: 30/60

SINR at a given position. Since our topology contemplates a MS in a given position (*x*,*y*), and given a BS transmitter power P_{Tx}, the MS at position (*x*,*y*) can be expressed by:

$$SINR(P_{Tx},x,y)=\frac{P_{ow}(P_{Tx},x,y)}{(1-\alpha)\cdot P_{ow}(P_{Tx},x,y)+P_{nh}(P_{Tx},x,y)+P_{noise}} \quad (3.3.13)$$

where: P_{ow} is the power received from the own cell, α is the orthogonality level of the codes according to [25], P_{nh} is the total amount of interfering power coming from the neighbor cells (6 cells in the case of hexagonal cell deployment), p_{noise} is the thermal noise power. The interference power received by a MS from the first ring of six neighbor cells is given by:

$$P_{nh}(P_{Tx},x,y)=\sum_{i=1}^{6} I_i(P_{Tx},x,y) \text{ with, } I_1{=}I_6, I_2{=}I_5, I_3{=}I_4 \quad (3.3.14)$$

where: $I_i(P_{Tx},x,y)=P_{Tx}G_{Tx}G_{Rx}10^{\frac{-PL(x,y)^i}{10}}$.

Average SINR in the cell. The average SINR within a cell is the SINR measured by a MS with uniform probability density function for its deployment over the cell area. It depends on the cell radius, *R*, and on the BS transmitter power, P_{Tx}, as follows:

$$\overline{SINR}(P_{Tx},x,y)=\frac{\overline{P}_{ow}(P_{Tx},x,y)}{(1-\alpha)\cdot \overline{P}_{ow}(P_{Tx},x,y)+\overline{P}_{nh}(P_{Tx},x,y)+P_{noise}} \quad (3.3.15)$$

The average interference generated by a neighbor cell can be calculated by integrating each fraction of the interfering power over the area of the affected cell. Figure 3.14 shows one cell affected by interference in the origin of the coordinates and one interfering cell, at (x_0, y_0). By integrating over the hexagonal cell area, the average level of the received power from a neighbor cell, $\overline{I}$, may be calculated as:

$$\overline{I}(R,P_{Tx})=\int_y\int_x f_I(P_{Tx},x,y)dxdy=\int_y\int_x \frac{P_{Tx}G_{Tx}G_{Rx}}{A_{cellnh}}PL(x,y)dxdy \quad (3.3.16)$$

where: A_{cellnh} is the total affected cell area. As the surrounding interfering neighbors are all at the same distance, $\sqrt{3}R$, $\overline{P}_{nh}(P_{Tx},x,y)=6\cdot\overline{I}(P_{Tx},R)$, as it is shown in Fig. 3.14.

$\overline{P}_{ow}(P_{Tx},x,y)$ is the average signal power within a cell and it is constant for the same frequency model, no matter what value of *K* is used.

Transmitter Power Normalization Procedure. The goal of the average SINR analysis is to determine a set of transmitter powers, P_{Tx}, to be considered in future simulations, in order to have a constant average SINR for all the cell radii. Figure 3.15 shows the average SINR results.

Layout: T1 Standard SC | Book ID: 318863_1_En | Book ISBN: 978-3-319-04021-9
Chapter No.: 3 | Date: 24-12-2013 | Page: 31/60

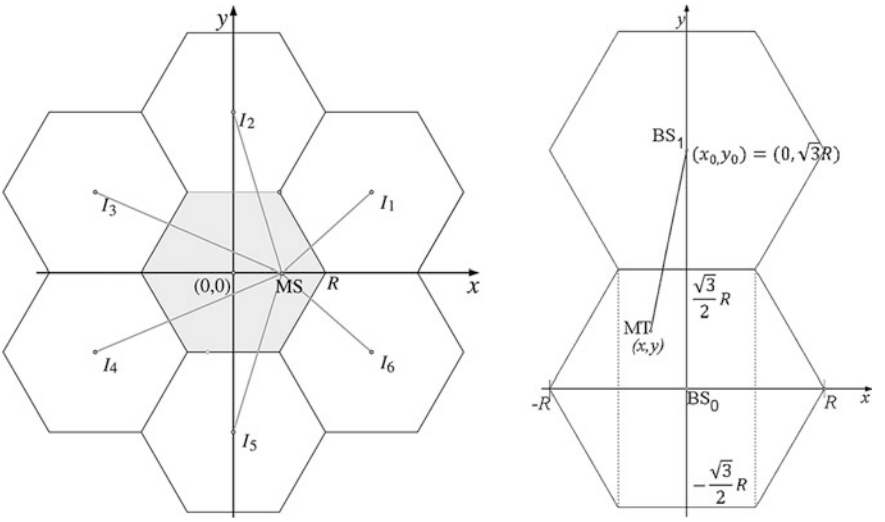

Fig. 3.14 Topology considered in our formulation with K = 1, the inter and intra cell interference for the HSDPA LTE network

Results. The performance of the SA user allocation is assessed by using the total Service Throughput (*Serv_thr*) metric which was discussed in "Results" of Sect. 3.3.1.2.

The system can achieve better performance if MSs are allowed to be switched between bands. Figure 3.16 shows the results in the presence of the iCRRM with the proposed GMBS algorithm, for several cell radii with normalized power. Due to the power normalization procedure, the performance of the iCRRM is almost constant for all the cell radii. In the saturation point, a gain of 30 % is achieved compared to the absence of iCRRM.

Figure 3.17 presents the throughput gain in percentage and the absolute gain as a function of the cell radius under a constant average SINR: the power normalization procedure proposed in the previous section allows for fair results comparison with variable cell radius. The almost constant gain demonstrates the potentiality of iCRRM over a wide range of cell coverage distances.

Figure 3.18 shows the load variation depending on the number of active MSs in the cell for both frequency bands and R = 300, 900 and 1,500 m. Since the path loss is lower at 2 GHz compared to the 5 GHz band, in the case of low cell load, the iCRRM entity will mainly allocate the MSs to the 2 GHz band.

Figure 3.19 presents the average PER as a function of the MS-BS distance for three cell radii: R = 300, 900 and 1,500 m; the use of iCRRM shows a significant reduction of PER, especially for the 5 GHz band.

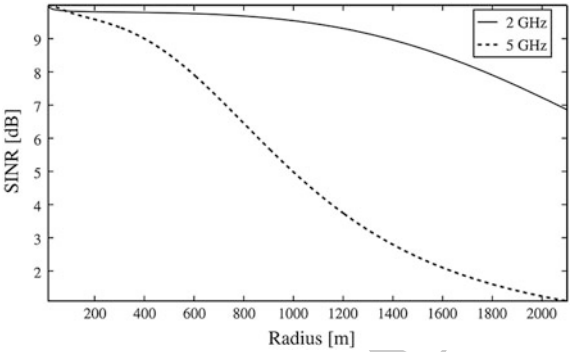

Fig. 3.15 Average SINR (dB) as a function of the cell radius [m]

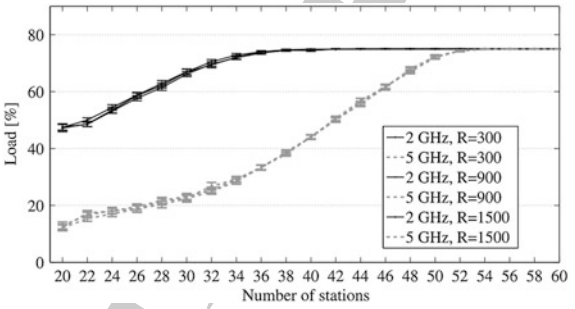

Fig. 3.16 Average service throughput with the iCRRM with normalized power

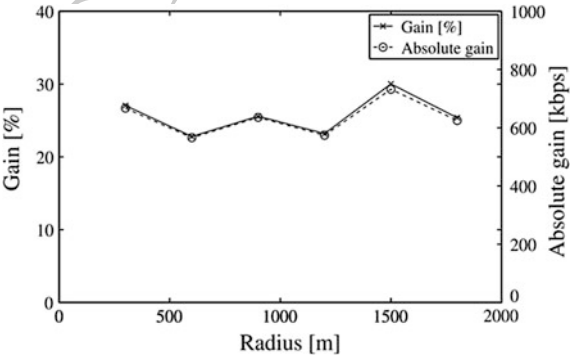

Fig. 3.17 Gain between the presence and absence of the iCRRM as a function of the cell radius

For all the cell radii, the GMBS is able to reduce the PER from 0.01 to 0.005 via an accurate selection of the MSs to be moved between 2 and 5 GHz, based on their channel quality in each frequency band.

Layout: T1 Standard SC | Book ID: 318863_1_En | Book ISBN: 978-3-319-04021-9
Chapter No.: 3 | Date: 24-12-2013 | Page: 33/60

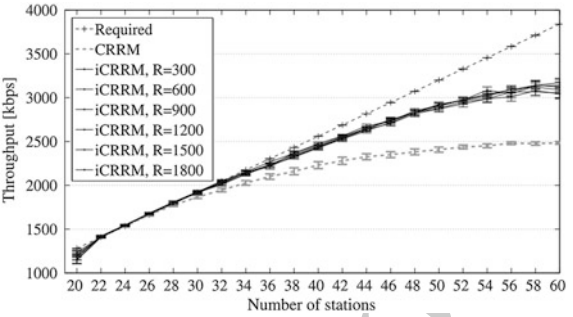

Fig. 3.18 Variation of the load with the number of SSs for 60 users for both frequency bands for R = 300, 900 and 1,500 m

3.3.3 *Transmitted Power Formulation for the Implementation of Spectrum Aggregation in LTE-Advanced Over 800 MHz and 2 GHz Bands*

An innovative formulation to compute the average SINR in the context of SA in LTE systems is proposed, which comprises an iCRRM entity from Sect. 3.3.2 and schedules the users between the two LTE systems operating at 800 MHz and 2 GHz, whilst considering the integer programming optimization and considering RR schedulers within each LTE system. Firstly, considering a topology with a frequency reuse pattern K = 3 and the COST-231 Hata model [26] for the path loss (L) for two carrier frequencies, 800 MHz and 2 GHz, we obtain the following L model:

$$\begin{aligned} L_{800\ \mathrm{MHz[dB]}} &= 119.6 + 37.2 \cdot \log_{10}(R_{[\mathrm{km}]}) \\ L_{2\ \mathrm{GHz[dB]}} &= 128.1 + 37.6 \cdot \log_{10}(R_{[\mathrm{km}]}) \end{aligned} \tag{3.3.17}$$

Following a similar approach as in Sect. 3.3.2, now working at 800 MHz instead of 5 GHz, the values for the transmitter power are found for different cell radii so that a constant average SINR could be kept. According to [25] (Chap. 12), for a topology with a MS in a given position $(y, 0)$ and for $K = 3$, the inter-cell BSs distance is $3R$, as it is shown in Fig. 3.20.

According to [27], for HSPA, $(1 - \alpha) \cdot P_{ow}(P_{Tx}, x, y)$ with $\alpha \in [0,1]$, denotes the average channel multipath orthogonality factor, i.e., the fraction of the total output power that is experienced as intra-cell interference as the channels from the same cell are no longer perfectly orthogonal. Furthermore, for HSDPA, $\alpha > 0.9$ is assumed most of the time, while for WCDMA values in the range [0.5, 0.9] are recommended. The LTE design from [27] proposes to assume unitary α for simplicity. Thus, for LTE, the own cell interference is not considered in Eq. (3.3.5) from section, due to the lack of codes, as in WCDMA/HSDPA systems.

Figure 3.21 shows the average SINR in both frequency bands with different BS transmitter powers and $\alpha = 1$, achieving the maximum values of 19.5489 dB and 19.8416 dB, for the 800 MHz and 2 GHz frequency bands, respectively. Finally,

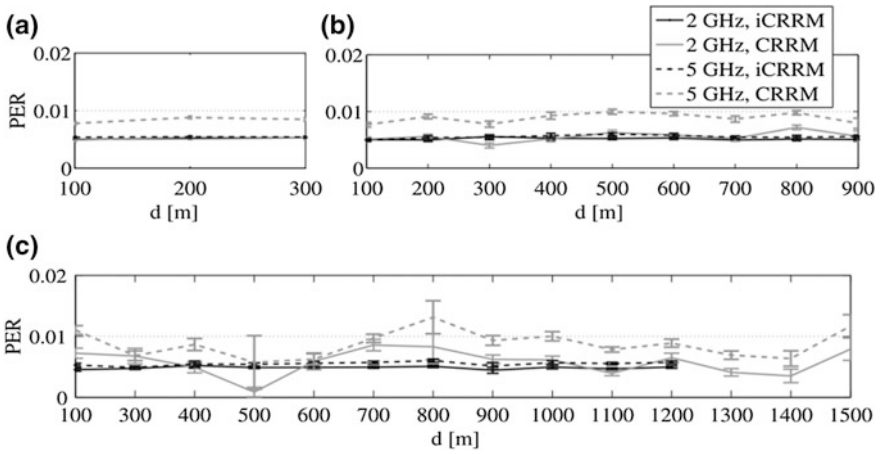

Fig. 3.19 PER variation for cell radii. **a** R = 300, **b** R = 900 and **c** R = 1,500 m

to calculate the normalized P_{Tx}, required in both bands (to maintain such an average SINR constant), we took $\overline{\text{SINR}}_{\text{max800MHz}} - V$ %, $-V$, where V is the percentage of variation. Table 3.3 shows the results of the normalized transmitter powers, P_{Tx}, required, with variation V equal to 1, 5 and 10 %.

Figure 3.22 shows that, as the cell radius increases, the transmitter power required to keep the envisaged average SINR constant increases as well.

3.3.4 Opportunistic Load and Spectrum Management for Mobile Communications Energy Efficiency

The power consumption of mobile and wireless communications systems can be quite significant. Even an environmentally-aware operator, such as Vodafone, consumes approximately 40 MW in running its business in the UK, the majority of which can be attributed to base stations (BSs) [28]. Lowering the operational power consumptions of BSs is particularly important. Enabling sleep modes for such equipment, and more generally reducing necessary transmission power, can have a very significant effect on the overall power consumption.

3.3.4.1 Power Saving Spectrum Management Concepts

Power Saving by Dynamically Powering Down Radio Equipment. The concept, illustrated in Fig. 3.23a, is the switching off of radio equipment through reallocating load to other bands at times of low load. This is extremely promising as it

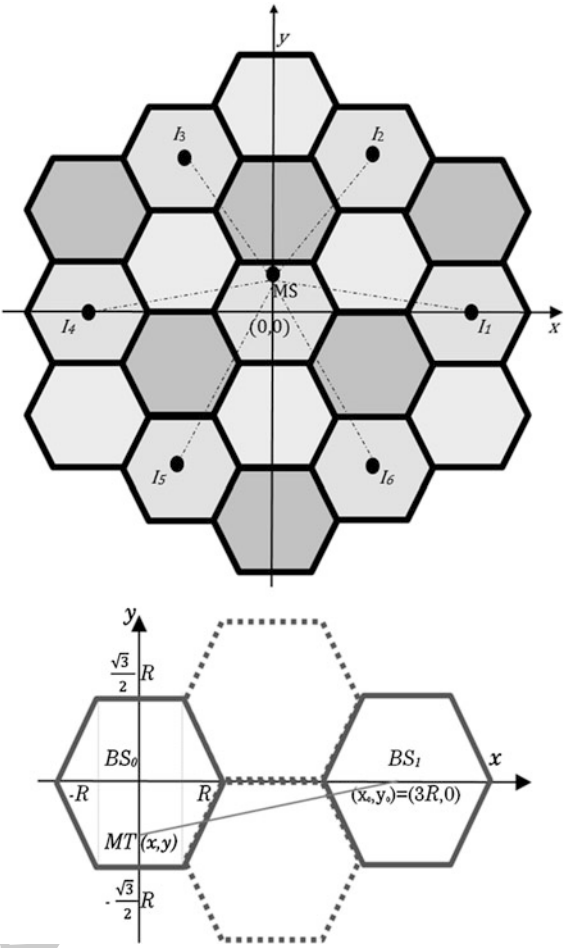

Fig. 3.20 Topology considered in our formulation with K = 3, the inter and intra cell interference for an LTE network

implies a guaranteed power saving through radio equipment being virtually "switched off at the socket".

There are two possibilities: (i) turning off cells entirely in one network or spectrum band at that time/location, through traffic being sufficiently carried by a single network or spectrum band, and (ii) using spare capacity of one network/band to cover the required drop in load of another network/band in order to enable that other network/band operate in omnidirectional mode instead of tri-sectored mode. The power saving assessments of this concept reallocates users between bands whenever possible to achieve one or both of these objectives.

Power Saving by Propagation Improvement.

The concept, illustrated in Fig. 3.23b, is the opportunistic reallocation of links or users to more appropriate propagation bands at times when that spectrum becomes

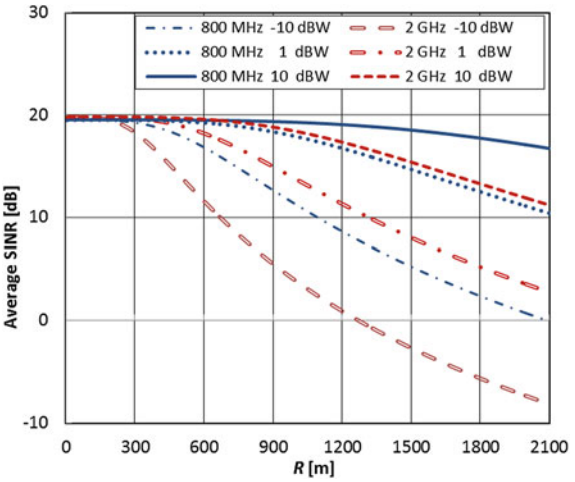

Fig. 3.21 Average SINR (dB) as a function of the cell radius (m) with three values of P_{Tx} (−10, 1 and 10 dBW)

Table 3.3 Values for the normalized transmitter power PTx (dBW) for the 800 MHz and 2 GHZ bands

V(%)	Freq. Band (MHz)	Radius (m)					
		300	600	900	1200	1500	1800
1	800	−1.971	9.226	15.777	20.424	24.029	26.975
	2000	5.951	17.263	23.883	28.580	32.224	35.201
5	800	−9.113	2.085	8.635	13.283	16.888	19.834
	2000	−1.064	10.253	16.874	21.572	25.215	28.193
10	800	−12.772	−1.575	4.976	9.624	13.229	16.174
	2000	−4.706	6.612	13.233	17.931	21.574	24.552

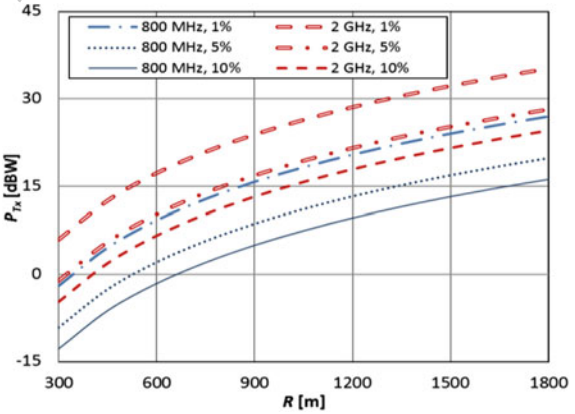

Fig. 3.22 Normalized P_{Tx} required to achieve a constant average SINR (dB), near the maximum, as a function of the cell radius at 800 MHz and 2 GHz

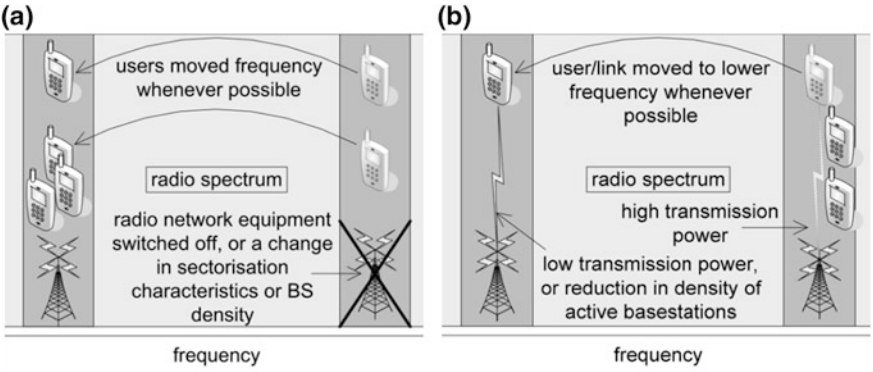

Fig. 3.23 Power saving concepts: **a** Reallocating traffic to enable radio network equipment to be switched off. **b** Reallocating users/links to improve propagation

available. This decreases necessary transmission power due to improved propagation, or alternatively in a frequency reuse scenario, reallocation based on the necessary deployed cell density/radius and the given local propagation environment can be used to reduce inter-cell interference through minimizing power "leaking" into co-channel cells. Both power saving concepts might be employed together, yielding further improvement in power efficiency.

3.3.4.2 Assessment of Power Saving Potential

Power saving potential of the aforementioned concepts is assessed through simulation of cellular systems carrying either video, FTP, or HTTP (web browsing) traffic. Concerning the traffic models used in simulations, it is assumed that the average cell load at time of day t, $L(t)$, varies according to a set of statistics on traffic load as a percentage of busy hour load (*BusyLoad*) over a 24 h period, pertaining to traffic in a 3G network in London, UK. Two simulation approaches are taken. In the first, it is assumed that the statistical number of active users in the cell receiving a video flow is Poisson distributed, the mean of which at any one time of day can be taken from the average load at that $L(t)$. The probability of there being k active users in the cell at time of day t is expressed as:

$$P(k,t) = \frac{L(t)^k e^{-L(t)}}{k!} \tag{3.3.18}$$

Under this first approach, our numerical assessment cycles in outer loops through a 24 h period in steps of t of one hour, and uses the value of $L(t)$ (given *BusyLoad*) at each hourly time unit to parameterize Eq. (3.3.1). In inner loops, for each time unit, it then cycles through each possible value of k representing each possible number of users in the cell, for all participating frequency bands, and for each set of k's ascertains the power consumption that would be required given

Layout: T1 Standard SC | Book ID: 318863_1_En | Book ISBN: 978-3-319-04021-9
Chapter No.: 3 | Date: 24-12-2013 | Page: 38/60

power saving solution being applied. The actual power consumption for each case is given as this power consumption, multiplied by the probability of it happening. This result is then summed with equivalent results for all possible chosen values of k to obtain the overall power consumption at time unit t. The same operation is performed over all hourly t in the 24 h period, and the average power consumption is then taken among all t. The same process is performed to find the average power consumption of a conventional system without the power saving operation being applied.

The second simulation approach assumes a separate ON/OFF traffic flow to each user, either parameterized as FTP or HTTP traffic, taken from [29], whereby the number of users receiving flows varies throughout the 24 h period according to $L(t)$.

3.3.4.3 Power Saving by Dynamically Powering Down Radio Equipment

Simulating the LTE system with video traffic sources to users, Fig. 3.24 gives the percentage of from-the-socket power ("Energy Reduction Gain—ERG") that is saved through moving users between bands to dynamically power down radio equipment, for 2, 3, and 4 spectrum bands participating in the process, where the 2-band case considers the network powering down solution with and without sectorization switching in tandem. For all results in Fig. 3.24 *BusyLoad* is the same for all channels. It is clear that power savings in the range of 20–50 % can be achieved if there are lesser bands participating in the process or there is a greater network loading. For the 2-band case, if the networks are heavily loaded the sectorization switching solution considerably improves performance compared with the network powering down solution operating alone, but offers no improvement if networks are lightly loaded.

Figure 3.25 plots power saving results for the FTP and HTTP (web browsing) ON/OFF traffic models over the LTE configuration, where 2 bands are participating in the process and the assumption is that the network powering down solution only is employed.

Results again show a significant power saving potential of up to 50 % for low network loads. In the FTP case, power saving begins to reduce at a *BusyLoad* of $\sim$20 users, reaching as low as 10 % at a *BusyLoad* of $\sim$50 users. In the HTTP case, power saving begins to reduce at a *BusyLoad* of $\sim$150 users, and hits 10 % at a *BusyLoad* of $\sim$500 users.

3.3.4.4 Power Saving by Propagation Improvement

In assessing the power saving of reallocating users/links to improve propagation, we have opted to study an HSDPA system. This is because an HSDPA BS was the most modern specification BS for which detailed data was available on from-the-

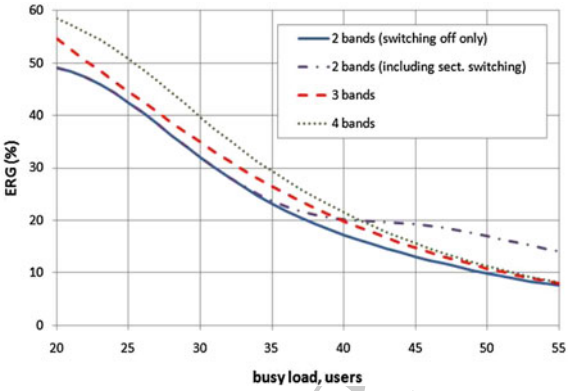

Fig. 3.24 Power saving against busy hour load for powering down solutions (streaming video traffic)

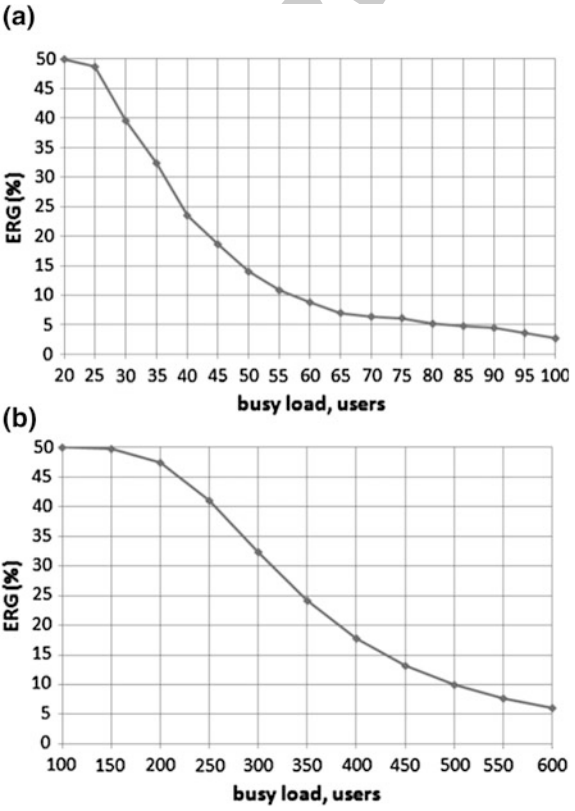

Fig. 3.25 Power saving against busy hour load for network powering down solution: **a** FTP ON/OFF traffic. **b** HTTP ON/OFF traffic

socket power consumption against transmission power. Internal documentation indicates power consumption for an HSDPA BS at 100 % transmission power to be 857 W, and at 20 % transmission power to be 561 W. It is widely observed that from-the-socket power consumption against transmission power broadly varies

Layout: T1 Standard SC | Book ID: 318863_1_En | Book ISBN: 978-3-319-04021-9
Chapter No.: 3 | Date: 24-12-2013 | Page: 40/60

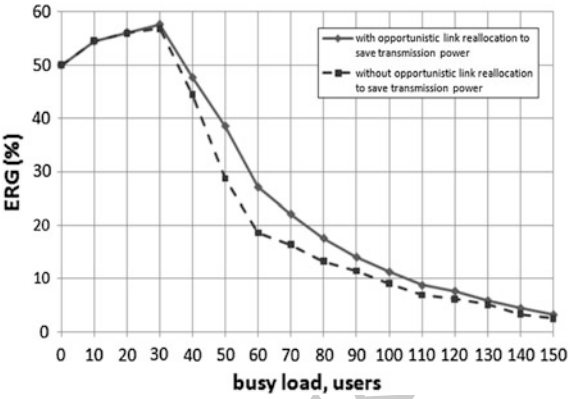

Fig. 3.26 Power saving against busy hour load through opportunistic link reallocation to use better propagation bands (FTP ON/OFF traffic)

with an $m \cdot p + c$ relationship, comprising a fixed term c that is independent of transmission power p, and a term that varies with transmission power, $m \cdot p$. The above figures regress to give 487 W, as the fixed part from-the-socket power consumption c, and the gradient of variation with transmission power m as 9.25 W per transmission Watt.

In ascertaining necessary transmission power, we use values in Table 3.3 of Ref. [30], with 80 % of the power budget scaled by the number of users present in the system and 20 % allocated to pilot transmission. The comparison in [30] is between full HSDPA networks operating at 2 GHz, and at 5 GHz. A 600 m cell radius is chosen, where again we assume the FTP ON/OFF traffic model. Figure 3.26 show that there is significant transmission power saving potential through the opportunistic reallocation scheme.

Power saving initially increases to some 58 % as the busy hour load is increased to 30; this is because it is always possible to reallocate users to power down radio equipment. However, as the traffic load is increased further power saving decreases and a difference begins to emerge in performance for the solutions with and without opportunistic reallocation to save transmission power.

3.4 Opportunistic Unsynchronized Cognitive Radio Networks Using Filter Bank Multicarrier (FBMC)

Maurice Bellanger

The Conservatoire National des Arts et Métiers (CNAM), Paris, France

The radio spectrum has two essential characteristics for communication, it is a limited resource which can be accessed from everywhere. The concept of cognitive radio has been created with the objective to make the best of this situation, by providing the highest spectral efficiency and offering the maximal access

flexibility. The ultimate implication of the concept is that a communication system, for example a base station and its users, which detect an unoccupied frequency band in the spectrum should have the freedom to exploit it, without having to go through a lengthy clearance procedure and coordinate with other systems in the same geographical area. Hence, the denomination of opportunistic unsynchronized networks. From the operational perspective, the approach is particularly appealing due to its potential agility and the possibility to use a light infrastructure.

In practice, however, the introduction of such new systems amid existing communication networks or broadcasting devices requires a minimal level of regulation and standardization, in order to ensure coexistence and gain acceptance by all the players in the field. In fact, it appears that some global supervision will be required, at least at the beginning of the spectrum sharing deployment process. To that purpose, the most promising technique is the geolocation data base concept, according to which the users receive relevant information about the spectral occupancy in their local environment and instructions for their operation conditions. Depending on the level of authority the data base will have on the users and its ability to impose connection parameters, the cognitive radio networks will be semi-opportunistic or not opportunistic at all.

In any case, truly opportunistic or not, the cognitive radio networks must rely on the capabilities of their terminals to face the challenge of maximizing spectral usage under the constraint of coexistence. The physical layer is particularly critical in that respect and it must have the following features:

- capability to handle unsynchronized users with minimal loss in spectral use. For example, primary and secondary users cannot be synchronized.
- guaranteed protection of other users, for coexistence.
- capability to exploit fragmented spectrum in case of broadband transmission.
- capability to establish a link without preliminary distant alignment, for multi-user efficiency.
- high performance for real time spectrum sensing/monitoring in terms of resolution and latency, for autonomous access decision or to complement the information provided by the geolocation data base.

Multicarrier transmission techniques have the potential to provide these features. However, the technique employed by existing systems, OFDM, does not fully satisfy the above requirements. An improved physical layer is needed and the FBMC technique is proposed for cognitive radio systems, as an enhancement of OFDM. The approach consists of complementing the FFT of the OFDM scheme by a set digital devices, called a polyphase network, so that a filter bank is obtained, in which a protype filter is shifted in frequency around the sub-carriers. Then, the transmission channel is split into a set of sub-channels and the attenuation characteristics of the prototype filter controls the spectral separation of the sub-channels. In order to minimize system latency and computational complexity, a sub-channel overlaps with its immediate neighbours, so that it is sufficient to introduce an idle sub-channel between two blocks of sub-channels to separate

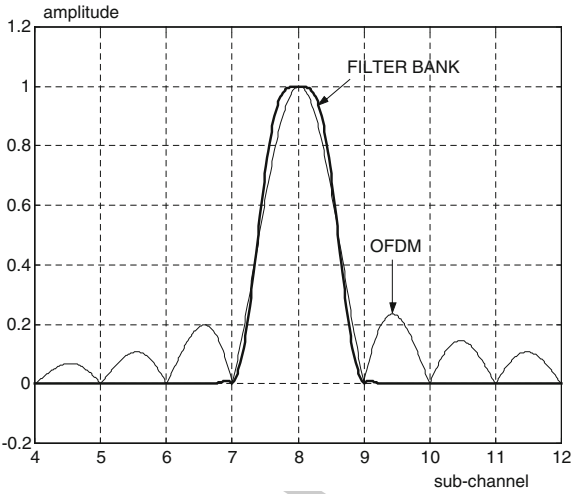

Fig. 3.27 Frequency responses of OFDM and FBMC

these blocks and make them spectrally independent. The comparison with OFDM is illustrated in Fig. 3.27. The OFDM frequency response exhibits large sidelobes so that full synchronization of the sub-carriers is necessary. The filter bank has no sidelobes, and only neighbouring sub-channels overlap.

As shown in Fig. 3.28, users with different transmission parameters may occupy the spectrum, even with different modulation schemes. Regarding spectral efficiency, there is no cyclic prefix, which means an increased bit rate and easy streaming. If necessary, for example in broadband communications, the distortions of the transmission channel can be compensated by equalizers at the sub-channel level.

Radio networks generally transmit by bursts. With FBMC, the transmission of a burst requires some extra time to accommodate the initial and final transitions associated with the filter impulse response. An illustration is given in Fig. 3.29. In fact, these transitions ensure that the adjacent users are not disturbed when a user accesses or quits the spectrum. If a frequency gap is present between the users or if a temporary reduction in performance is tolerable, the transitions can be significantly shortened, for example to $Ns + 1$ symbols if Ns symbols have to be transmitted. The practical consequence of the increase of the burst length is that FBMC favours longer bursts.

In any case, when compared with the OFDM burst, the FBMC burst carries more data symbols in a given time interval, because there is no guard time, or cyclic prefix, between the multicarrier symbols.

The filter bank in the receiver can also be employed for spectrum sensing and the conventional techniques can be applied at the sub-channel level, namely energy detection, matched filter, cyclostationarity feature detection or self-correlation. The specificity of FBMC lies in the spectral separation provided by the filters and the absence of spectral leakage which improves the performance. In particular, significant gains can be obtained with respect to OFDM concerning

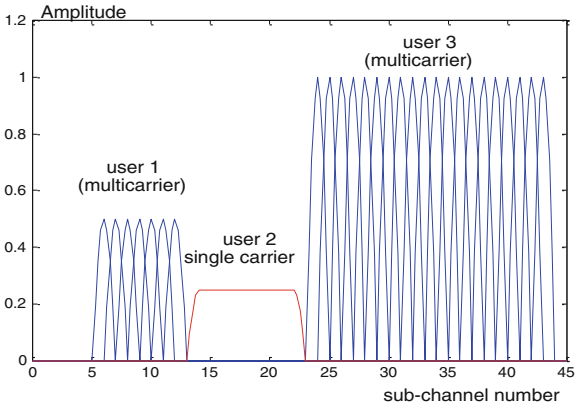

Fig. 3.28 Multi-user transmission with FBMC

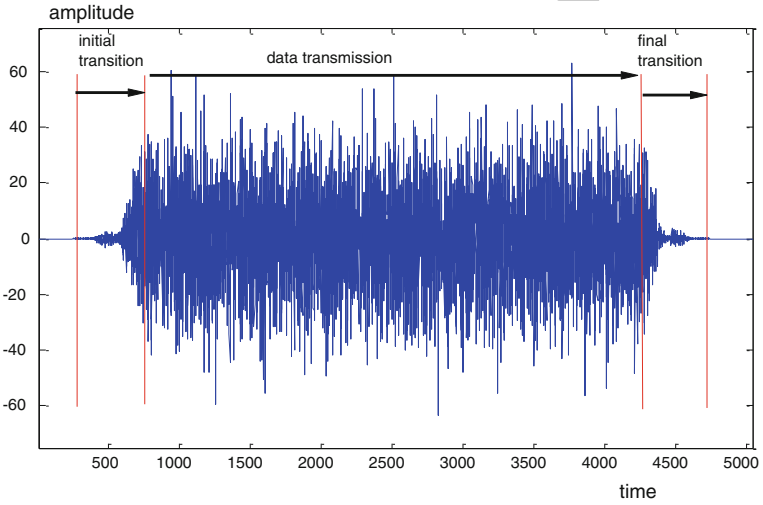

Fig. 3.29 Structure of the transmitted burst with FBMC

noise power estimations. The counterpart is the latency, in which the filter impulse response must be included.

An important aspect is that continuous spectrum monitoring is readily achieved if sub-channels are reserved for this function. In particular, if a group of 3 sub-channels is left idle, the center sub-channel does not overlap with the active sub-channels and it can sense during transmission.

Finally, it can be stated that a system based on the FBMC physical layer can operate efficiently in an unsynchronized environment. The next step towards building the opportunistic or semi-opportunistic network is the definition of a suitable protocol.

Layout: T1 Standard SC | Book ID: 318863_1_En | Book ISBN: 978-3-319-04021-9
Chapter No.: 3 | Date: 24-12-2013 | Page: 44/60

3.5 Detection of Malicious Users in Cognitive Wireless Ad-Hoc Networks: A Statistical Approach

Ferran Adelantado[1] **and Christos Verikoukis**[2]

[1]Universitat Oberta de Catalunya, Barcelona, Spain
[2]Telecommunications Technological Centre of Catalonia (CTTC), Barcelona, Spain

The Opportunistic Spectrum Sharing (OSS) concept [31] is based on two main premises: the maximization of the spectrum usage and the protection of the incumbent primary systems. Both premises are highly coupled and depend on the accurate knowledge of the nearby wireless environment, i.e. the detection of primary users (PU) transmitting/receiving in the vicinity of the secondary users (SU).

The research community is currently debating between two cognition approaches: the local sensing [32] and the usage of location databases [33]. The former is based on the acquisition of spectrum usage knowledge by sensing the air interface whether in a cooperative or non-cooperative manner. On the contrary, the latter assumes the existence of a spectrum usage database, which is updated periodically by the PUs, where all SUs address queries before leasing any primary channel. If, for a given SU location, time, and spectrum resource, the database response certifies the idleness of the PUs, the SUs lease the spectrum. Each approach is deemed appropriate for different applications.

Focusing on the local sensing approach, it relies on the sensing capabilities of the so-called Secondary Users (SU). Usually, SUs are assumed to be able to detect and identify the energy transmitted by the primary Users (PU), process the information and proceed accordingly [31]. However, such capabilities are limited in nature and the SUs present non-null false alarm and missed detection probabilities [32]. Both inadequacies, i.e. false alarm and missed detection, affect the two premises on which OSS is based. Whereas false alarm diminishes the spectrum usage efficiency, missed detection endangers the protection of the incumbent PUs. In the aforementioned context, the cooperation among SUs comes up as a proper manner to improve the environment knowledge obtained during the sensing process [34]. However, although cooperation is effective to smooth the effect of sensing errors, it turns out to be inefficient to cope with the attacks of malicious SUs [35, 36]. Thus, cooperation poses new vulnerabilities, since false information might be easily propagated across the secondary network. In order to limit the impact of inaccurate/false sensing information, malicious SUs detection mechanisms are required.

In this section, a new algorithm based on statistical non-parametric methods is proposed to detect the malicious SUs. First, it is worth noting that any detection mechanism should consist of two stages:

Detection of the existence of malicious SUs: In the first stage, given a set of users, it must be decided whether there are malicious SUs or not.

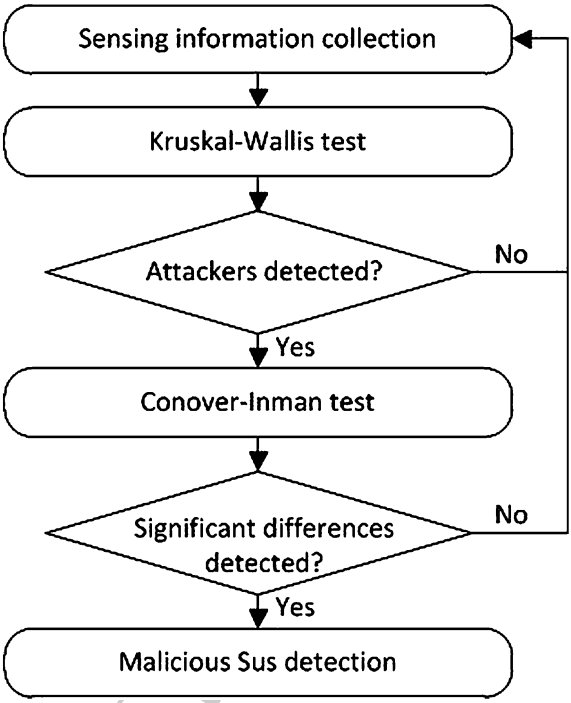

Fig. 3.30 Flowchart of the detection mechanism

Identification of the malicious SUs: Given a set of users where at least one of them is malicious, in the second detection stage the malicious SUs must be identified.

In the context of cognitive wireless ad-hoc networks, the assumptions regarding the knowledge of the primary channel activity have a huge impact on the feasibility of the proposals. Hence, there are two hypotheses that limit the real application of the detection mechanisms: the knowledge on the existence of malicious SUs and the knowledge of the primary channel activity.

In the system under study, the detection of malicious users can be done by comparing the sensing information provided by the cooperative SUs. As little a priori information is known about the behavior of the SUs, non-parametric statistical methods are appropriate to effectively perform such a task. In particular, the Kruskal–Wallis [37] analysis is used to detect the existence of attackers, whereas, after detecting it, the post hoc Conover-Inman [38] analysis is aimed to identify the malicious users. The flowchart of the process is shown in Fig. 3.30.

The described mechanism has proven to detect the malicious users even when there is not a priori information regarding the activity of the primary channel and the characteristics of users. Yet, it is also true that the optimum performance of the proposed mechanism depends a great deal on its parameters, e.g. the number of employed samples or the significance level, which should be tuned according to the scenario characteristics.

Layout: T1 Standard SC | Book ID: 318863_1_En | Book ISBN: 978-3-319-04021-9
Chapter No.: 3 | Date: 24-12-2013 | Page: 46/60

3.6 Spectral Efficiency for the Benefit of CR and Coexistence with Iterative Water-Filling

Maurice Bellanger

The Conservatoire National des Arts et Métiers (CNAM), Paris, France

3.6.1 Efficiency and Coexistence

Waterfilling (WF) improves the spectral efficiency of communication systems whenever the channel signal-to-interference-plus-noise-ratio (SINR) exhibits large variations in the exploited frequency band. In radio communications, it can be applied to broadband transmission, provided the channel remains nearly static or varies slowly.

The WF technique, associated with multicarrier transmission, is implemented in several steps. The first step is the measurement of the channel SINR as a function of frequency, with the granularity of the multicarrier scheme. Then comes the bit-loading assignment, whereby the measurement results are used to distribute the number of bits to be transmitted in every symbol across the sub-carriers. The rule is that the sub-carriers carry a number of bits related to their received SINR. Specifically, the curve of inverted SINR is filled with energy, namely the sum of the received signal power and noise power, up to a constant level, hence the term "waterfilling". With this procedure, sub-carriers with high SINR receive more energy and carry several bits, while sub-carriers with low SINR receive less energy and carry a single bit or are just discarded. If the total number of bits per multi-carrier symbol is imposed, then the emitted signal power is adjusted, along with the "water level". Conversely, if the emitted signal power is specified, then the bit rate is adjusted. Next, once the bit loading has been decided, the information is forwarded to the distant terminal for implementation. Of course, for the procedure to be successful, the channel characteristics should not change significantly between successive symbols and, in any case, the roundtrip transmission delay of the system must be kept minimal. Also, it must be pointed out that the accuracy of the SINR measurements is critical for the benefit of the approach.

In fact, the WF algorithm is optimal for the radiated power distribution, in case of single user communication. Therefore, WF contributes to the efficiency of the spectrum usage.

Now, in the context of cognitive radio and multiple users, WF helps coexistence because the signal of a primary user, or that of another secondary user, will be incorporated in the global SINR measurement of a potential new secondary user and the overlapping sub-carriers are likely to be either not loaded at all, or weakly loaded. In other words, the WF procedure automatically leads to separating successive users in the spectral domain. Moreover, the fact that WF leads to the minimum of radiated power for a specified bit rate is an important contribution to

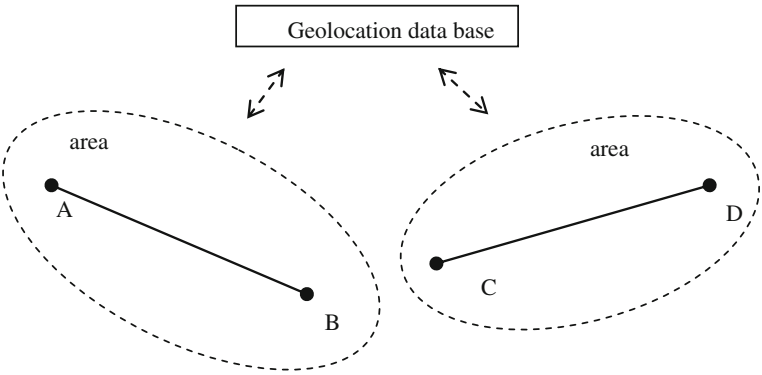

Fig. 3.31 Configuration with 2 secondary users

coexistence. Finally, it can be stated that modems, when they are equipped with WF algorithms and devices, autonomously adapt their power and spectra for coexistence.

Now, after the single modem case, the global behaviour of a system consisting of several modems implementing simultaneously and independently the WF technique is investigated.

3.6.2 Iterative Waterfilling

In order to simplify the analysis of the iterative process and obtain meaningful results, the system configuration is restricted to 2 opportunistic links, a specific yet representative scenario is defined and the global behaviour is explored by simulation.

The configuration is illustrated in Fig. 3.31. Links L1 and L2 operate in separate areas, area 1 and area 2 respectively. They are of opportunistic nature and they have to transmit for limited times, at specified rates. It is assumed that a regional geolocation data base has given the following authorizations

- L1 can transmit in the frequency band [F1, F2] with maximum radiated power P1max.
- L2 can transmit in the frequency band [F3, F4] with maximum radiated power P2max.

The frequency bands overlap ($F1 < F3 < F2 < F4$) and no direct connections exist between the two opportunistic links.

The iterative process is described as follows:

Layout: T1 Standard SC | Book ID: 318863_1_En | Book ISBN: 978-3-319-04021-9
Chapter No.: 3 | Date: 24-12-2013 | Page: 48/60

- *Stage 1*: L1 transmits the bit rate R1 in the band [F1, F2], using WF to cope with the channel distortion H1(f) and noise level N1. The radiated power needed is P1 < P1max.
- *Stage 2*: L2 begins transmitting the bit rate R2 in the band [F3, F4] using WF to cope with the distortion H2(f), the noise level N2 and the power generated by L1 in the overlapping band [F3, F4].
- *Stage 3*: L1 reacts to the arrival of L2 in a section of its spectrum and reduces the bit loading in the overlapping spectrum.
- *Stage 4*: L2 adjusts the bit loading to benefit from the improved spectrum in the overlapping band [F3, F2].

In the simulations, the parameters are varied and the convergence of the iterative process is examined. The performance of the individual links is assessed, and the global benefit of the iterative process is pointed out.

3.6.2.1 Conclusions

This section describes the conditions for WF to be beneficial and worth implementing at the individual link level, explained in terms of spectral efficiency and system coexistence.

The context and the conditions for iterative WF to bring noticeable gains in global performance and coexistence of opportunistic secondary users are presented.

The impact of WF on the exchanges between the individual links and the regional geolocation data base is discussed.

3.7 Assessing the Amount of Spectrum that may be Available for DSA

3.7.1 Technology Enablers for Spectrum Assessment: Radio Environmental Maps (REM)

Liljana Gavrilovska and Vladimir Atanasovski

University Ss. Cyril and Methodius, Skopje, FYR of Macedonia

The problem of re-usage of available spectrum opportunities faces difficult practical challenges because of the spatio-temporal and contextual dependence of the available spectrum. The theoretically envisioned Dynamic Spectrum Access (DSA) and Cognitive Radio (CR) solutions require novel, environment-aware and

self-organizing capable, approaches towards practical implementations in order to tackle the aforementioned challenges. The Radio Environmental Maps (REMs) [39–42] represent powerful technical enablers of DSA and CR. They were originally envisioned as a two-dimensional representation of the radio field strength [39], but today are foreseen as a rich hierarchical database or knowledge base that stores various kinds of radio environmental information. This information can be subsequently used for a plethora of optimization procedures in different DSA and CR scenarios [43].

REMs can store various type of information that can be easily fetched and used for a particular use-case. Generally, the stored information can be classified as either being *directly measured* (i.e. empirical) or being *indirectly derived* (i.e. derived through modelling). In any case, the information can be viewed (from a DSA and CR perspective) as:

- *Static*, e.g. locations of transmitters and/or receivers, terrain model etc. and
- *Dynamic*, e.g. propagation environment, up-to-date spectrum measurements, users' activity patterns etc.

The REM information can be used by many entities requiring reliable spectrum assessment. For instance, regulators and dedicated public bodies can use REMs for large-scale estimation of spectrum usage in order to track compliance to regulations, estimate frequency-planning effectiveness etc. Cellular network operators can interpret measured results through drive tests or mobile subscribers in order to perform Minimization of Drive Tests (MDTs), network planning and fault detection etc. Finally, consumers can perform self-optimization and/or learning of patterns and habits leading to higher QoS, lower prices etc.

The focal point of every REM is the capability to accurately assess the spectrum occupancy, i.e. accurate decision upon possible spectrum opportunities. As a result, the available spectrum opportunity detection techniques strongly influence the design and practical implementation of a REM. Currently, there are two distinct spectrum opportunity detection techniques [44], i.e.:

- Sensing-based spectrum opportunity detection and
- Database-based spectrum opportunity detection,

each with its own advantages and disadvantages [11]. The optimal way towards practical REM implementation should encompass features of both techniques [43, 45].

Figure 3.32 depicts the FARAMIR REM architecture [45] as the world's first complete practically deployed and fully operational REM creation architecture.

It comprises four distinguished architectural elements:

- **Measurement Capable Devices (MCDs)—**responsible for performing spectrum measurements (continuous and on-demand) in different band of interest.
- **REM data Storage and Acquisition unit (REM SA)—**responsible for storing the spectrum measurement data coming from the different types of MCDs, as well as information about the positions and configuration of radio transmitters and receivers, environment characteristics and REM processed data.

Layout: T1 Standard SC | Book ID: 318863_1_En | Book ISBN: 978-3-319-04021-9
Chapter No.: 3 | Date: 24-12-2013 | Page: 50/60

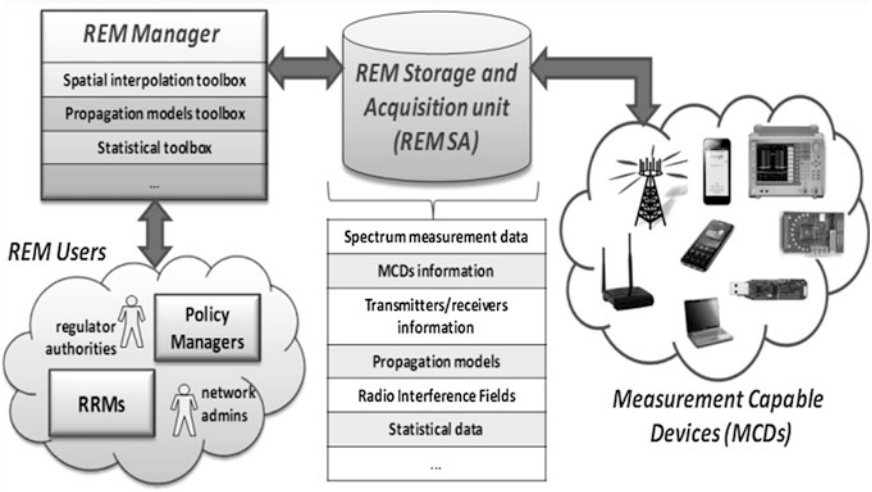

Fig. 3.32 The developed functional REM architecture [43, 44, 46]

- **REM Manager**—responsible for processing regarding the REM data creation and evaluation (modularly constituted comprising various toolboxes that serve for estimation of Radio Interference Fields (RIFs), localization of transmitters, statistical analyses of the spectrum usage, assessment of the environment propagation characteristics etc.).
- **REM Users**—entities that use the REM information, i.e. entities that govern the frequency/power allocation, spectrum access/(re-)usage, network optimization etc.

An example of the FARAMIR REM's architecture capability to act as technology enabler for spectrum assessment is its *spatial interpolation capability of sparse spectrum measurements* [42, 43, 45, 46] and its *transmitter localization capability* [47]. Both capabilities are embedded in the REM Manager as scalable toolboxes able to run real-time spectrum occupancy analysis. The spatial interpolation toolbox relies on local neighborhood based spatial interpolation whereas the transmitter localization toolbox uses an ML-like technique to detect potential transmitter fast and with sufficient accuracy. Figure 3.33 visualizes the obtained REM information for a particular case of using 16 independent heterogeneous spectrum sensors indoor and performing spatial interpolation in 900 points.

Additionally, the figure also shows other possible REM related functionalities such as real-time monitoring of the current signal strength level from every MCD in the field, real-time calculation of the duty cycle of a particular MCD for a given time frame and a given threshold of interest and statistical analysis of the field.

Layout: T1 Standard SC | Book ID: 318863_1_En | Book ISBN: 978-3-319-04021-9
Chapter No.: 3 | Date: 24-12-2013 | Page: 51/60

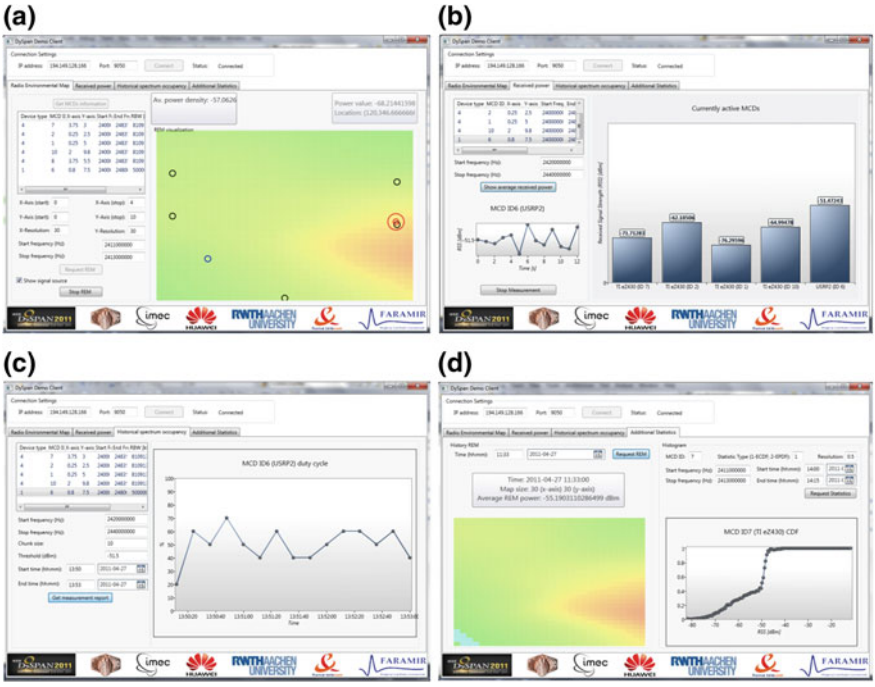

Fig. 3.33 Visualization of the REM information. **a** REM with MCDs and estimated transmitter's position. **b** Current Received Signal Strength (RSS) values for a single and multiple MCDs, **c** Calculated duty cycle for selected MCD, **d** Old REM and statistics graph

3.7.2 White Spaces Potentially Available in Italian Scenarios Based on the Geo-Location Database Approach

Marina Barbiroli[1], **Claudia Carciofi**[2], **Doriana Guiducci**[2] **and Valeria Petrini**[1]

[1]Bologna's University, Bologna, Italy
e-mail: marina.barbiroli@unibo.it; valeria.petrini@unibo.it
[2]Fondazione Ugo Bordoni, Rome, Italy
e-mail: ccarciofi@fub.it; dguiducci@fub.it

The estimation of the amount of spectrum potentially available as white space depends on several factors, as the White Space Device (WSD) characteristics, the topology of the area, the national rules governing the use of spectrum, the applications or services using the adjacent bands, and many others: these factors have to be fully defined by national or international regulators.

Spectral resources potentially available for White Space Devices (WSDs) in the UHF band (channels from 21 to 60) have been investigated by FUB [48] in the framework of the CEPT SE43 work group [49] based on the geo-location database approach [50].

Layout: T1 Standard SC | Book ID: 318863_1_En | Book ISBN: 978-3-319-04021-9
Chapter No.: 3 | Date: 24-12-2013 | Page: 52/60

Three different methodologies are implemented to estimate the amount of potentially available white space in different Italian scenarios [51].

3.7.2.1 Threshold-Based Approach for the Population of the Geo-Location Database

A first simple methodology to identify spectrum potentially available as white space is based on a threshold approach: in a specific location the received signal power on each channel is evaluated by means of a proper propagation model [52], and if the estimated power on a channel is below a selected threshold it is deduced that there are no licensed users for that channel in the proximity of the investigated location. Therefore a WSD is allowed to transmit its signal, provided that the specific emission requirements are met [53, 54]. The threshold can be determined as a function of different parameters such as the incumbent service to be protected (e.g., DTT, PMSE) or the level of protection to be granted.

The WS estimation based on a threshold approach has been performed as follows:

1. compute the power received on a given channel and in a given pixel (e.g. 600×600 m^2) by a receiving antenna (e.g. omnidirectional with 0 dBi gain) assumed at a specific height above ground level.
2. compare the received power against a specific threshold;
3. if the received power is below the threshold, the channel is considered as vacant;
4. iterate steps 1–4 for all the channels from 21 to 60 and for all the pixels of the considered area.

3.7.2.2 Location Probability Approach for the Population of the Geo-Location Database

The second approach is particularly focused on the protection of the DTT service which is the one of paramount interest for the Italian scenario. According to this approach, the usage of a specific channel is prevented within the coverage area of each DTT transmitter employing that channel, in order to guarantee a wanted Location Probability related to the proper field strength threshold [55]. In Table 3.4 the minimum median received field strength levels of the GEO-06 RPC at 650 MHz frequency are shown for fixed reception with respect to different location probability values.

DTT field strength levels are evaluated using accurate propagation models, which take into account also diffraction phenomena. Predicted values are then employed to identify the DTT protection area and the paired zone outside the coverage area where the channel is potentially available for WSDs.

Table 3.4 DTT reference planning configurations (fixed reception, frequency 650 MHz)

Location probability (%)	$F_{k,min}$ dBμV/m at 10 m
99	60
95	56
50	48
1	34

The potentially available white spaces are calculated based on the following approach:

1. for each pixel and for each channel, the field strength level E_{rx} (dBμV/m) considering all possible DTT transmitters is evaluated with a suitable propagation model;
2. the calculated field strength level E_{rx} is compared with the selected planning configuration threshold $F_{k,min}$ [55].
3. if E_{rx} is $> F_{k,min}$ the pixel is within the protected service contour, hence the channel is occupied; if E_{rx} is $< F_{k,min}$ the pixel is outside the protected service contour, hence the channel is vacant.

3.7.2.3 Combined Geo-Location Database and Sensing Approach

In this approach geo-location database and sensing methodologies are combined to determine white spaces potentially available.

Vacant and occupied channels are evaluated based on the following algorithm:

1. apply the methodology described in section B to identify white spaces (pixels and frequencies) potentially available based on the geo-location approach;
2. implement field strength measurements in different pixels and channels and compare the results with a proper sensing threshold to identify occupied and un-occupied channels;
3. only when "un-occupied channels" are obtained from both step 1 and step 2 the considered pixel and frequency are potentially available for the WSD otherwise the channel is occupied.

3.7.2.4 Threshold-Based Approach Results

We apply the estimation procedure described in section A to the case of West Piedmont. Using public information on ERP values and positions of each DTT transmitter, we assessed the power received in each channel and location by means of the Recommendation ITU-R P.1546-3 [52] assuming the receiving antenna height at 1.5 m and 10 m.

We considered two different thresholds set to −114 dBm and −120 dBm.

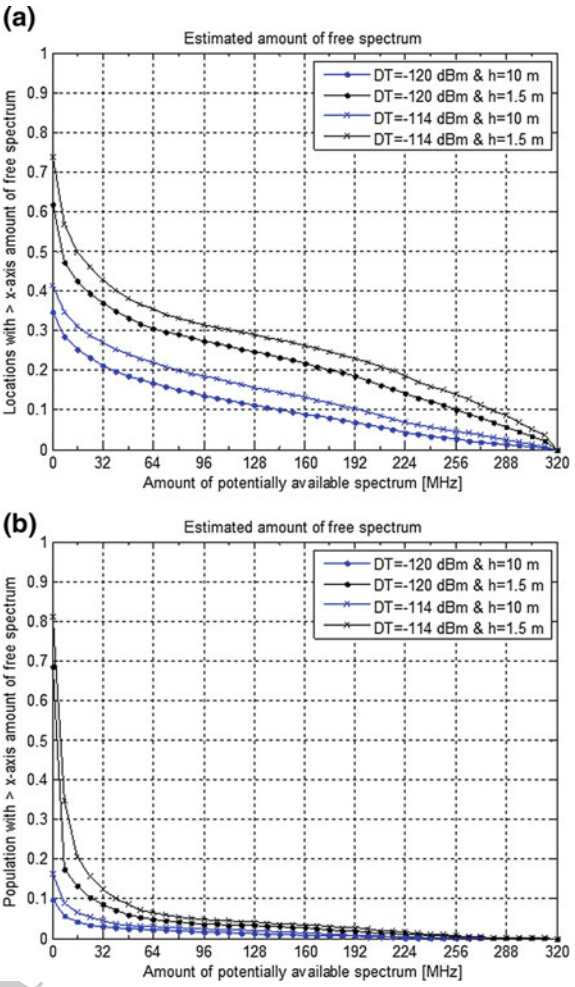

Fig. 3.34 Cumulative distribution function of the amount of White Spaces per pixel **a** and per population **b** (West Piedmont)

Figure 3.34a and b show the Complementary Cumulative Distribution Function (CCDF) of the estimated amount of spectrum available as white space respectively as a function of the territory and population density.

These figures confirm that densely populated areas have little or no spectrum available as white space since the areas where there are more available channels are rural. It can be easily noted that the CCDF referring to the population percentage (Fig. 3.34b) has a steeper descent than the one referring to the location percentage (Fig. 3.34a). For example, while almost 20 % of locations have more than 64 MHz available with DT = −120 dBm and h = 10 m, only 2 % of population actually resides in these areas. The amount of spectrum available as white space strongly depends on the chosen threshold. For instance, assuming a threshold equal to −120 dBm and an antenna height of 1.5 m, the percentage of

Layout: T1 Standard SC | Book ID: 318863_1_En | Book ISBN: 978-3-319-04021-9
Chapter No.: 3 | Date: 24-12-2013 | Page: 55/60

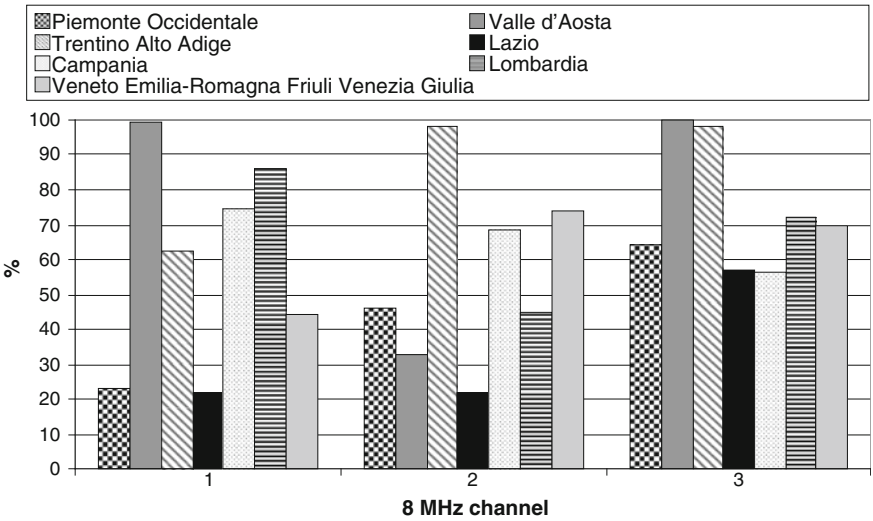

Fig. 3.35 Percentage of population living in potential white space areas for three different channels in several Italian regions

pixels where there is at least 1 available channel is 47.19 %, while raising the detection threshold to −114 dBm this percentage becomes 56.99 %.

Although these results refer to a delimited area of Italy, a similar behaviour is observed in other studies on EU and non-EU countries [56–57].

3.7.2.5 Location Probability-Based Approach Results

DTT coverage simulations have been performed in a real scenario in other different Italian regions. Predictions have been carried out using a proprietary prediction tool, where the propagation model takes also into account the diffraction phenomena according to ITU-R Recommendation P.526 [58]: occupied and vacant DTT channels are identified according to different levels of protection of the incumbent service (i.e., different percentage of Location Probability).

According to the adopted criteria for DTT protection, it is possible to identify those pixels where specific channels could be available for WSDs.

In Fig. 3.35 the usage of three different DTT channels in some Italian regions is considered and the percentage of population living in the white space locations is calculated on a regional basis. It can be noticed that there are regions where the chosen channels are almost completely un-occupied (e.g. mountain regions such as Valle d'Aosta and Trentino Alto Adige), while in more densely populated areas (e.g. Lazio) the considered channels are potentially available to serve a lower percentage of population.

Layout: T1 Standard SC | Book ID: 318863_1_En | Book ISBN: 978-3-319-04021-9
Chapter No.: 3 | Date: 24-12-2013 | Page: 56/60

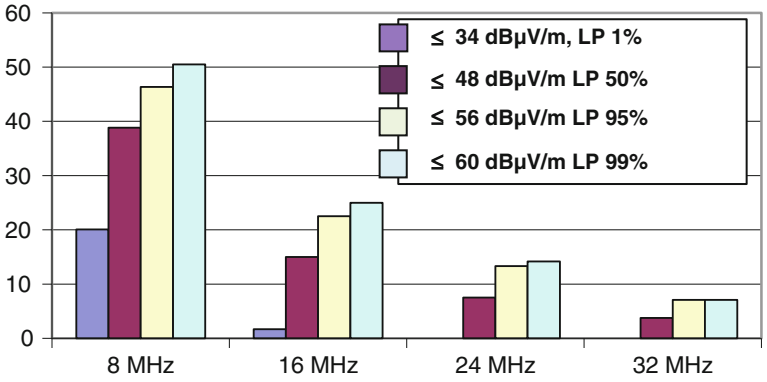

Fig. 3.36 Percentage of locations where 1, 2, 3 or 4 adjacent channels could be available

In Fig. 3.36 the percentage of locations where a least one or two or more adjacent DTT channels could be available in a central-north Italian region is calculated as a function of the protection level of the incumbent service.

It can be noticed that the percentage of locations where more bandwidth is potentially available strongly decreases as the number of the considered adjacent channels increases. Moreover the selected protection level for the DTT service has a strong impact on the percentage of locations where one or more channels could be available.

3.7.2.6 Combined Sensing and Geo-Location Results

The combined sensing and geo-location approach has been applied in a real scenario in Italy, in the province of Bologna. In the considered scenario field strength levels for DTT channels from 21 to 60 are calculated over square pixels (400×400 m^2). In Fig. 3.37 simulated field strength levels (dBμV/m) are shown for a DTT channel and it can be noticed that most of the pixels of the province of Bologna are occupied, as only some hilly and mountainous areas quite far from Bologna are not reached by the DTT signal.

Further information on channel occupancy can be achieved by means of sensing techniques. To this aim measurements have been implemented in six different locations using the "channel power" mode, in order to evaluate the total amount of power received in the DTT channel bandwidth.

In Table 3.5 the percentage of channels for which both geo-location database and sensing identify unoccupied channels is reported.

It can be noted that the percentage of potentially available WS is strongly dependent on the DTT protection threshold used to populate the geo-location database.

A comparison between results obtained with the combined approach and with the geo-location database alone highlights that the percentage of WS is similar

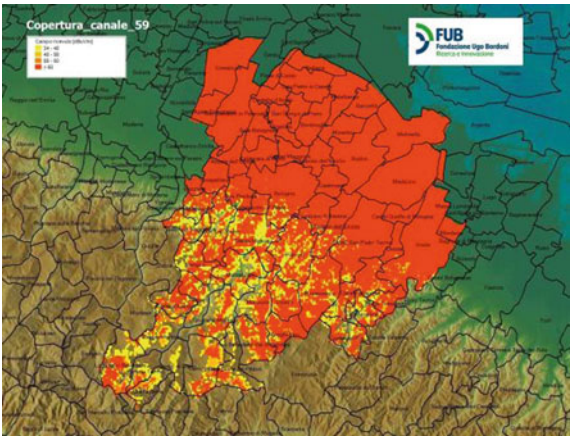

Fig. 3.37 Example of received DTT signal strength in the province of Bologna

Table 3.5 Combined geo-location and sensing approach

Different field strength levels for DTT reference planning configurations (fixed reception) dBμV/m	Percentage of available WS
<=34	20.08
<=48	38.89
<=56	46.15
<=60	50.43

considering the geo-location database alone and the combined geo-location database and sensing approach. This is mainly due to the scarce sensitivity of the probe equipment (−80 dBm) with respect to the sensing detection threshold specified in [59] (e.g. −120 dBm). Therefore to improve the accuracy of the combined approach we will provide other measurements with a probe which is characterized by a more accurate sensitivity level (<−80 dBm).

3.7.2.7 Conclusions

Some general considerations and remarks can be derived from the obtained results: we have applied different approaches to identify potentially available white spaces in real Italian scenarios. From simulation results, it is evident that in Italy the 470–790 MHz band is densely utilized and most of the potentially available WS are located in low populated zones such as mountain or hilly areas. Higher degree of the protection of the incumbent service strongly reduces the amount of unoccupied channels especially if contiguous bandwidth is needed to achieve

Layout: T1 Standard SC | Book ID: 318863_1_En | Book ISBN: 978-3-319-04021-9
Chapter No.: 3 | Date: 24-12-2013 | Page: 58/60

broadband WSD transmission. Moreover, the above analysis confirms that a combined geo-location and sensing approach may give higher protection to incumbent services, provided that a proper detection threshold is applied.

References

1. Report ITU-R SM.2152. Definitions of Software Defined Radio (SDR) and Cognitive Radio System (CRS). International Telecommunication Union (2009)
2. CEPT Report 24. Technical considerations regarding harmonisation options for the Digital Dividend. A preliminary assessment of the feasibility of fitting new/future applications/services into non-harmonised spectrum of the digital dividend (namely the so-called "white spaces" between allotments). Electronic Communications Committee (2008)
3. ECC Report 159. Technical and operational requirements for the possible operation of cognitive radio systems in the 'white spaces' of the frequency band 470–790 MHz. Electronic Communications Committee (2011)
4. ECC Report 186. Technical and operational requirements for the operation of white space devices under geo-location approach. Electronic Communications Committee (2013)
5. Draft ECC Report 205. Licensed shared access. Electronic Communications Committee (2013)
6. ECC Report 185. Complementary Report to ECC Report 159. Further definition of technical and operational requirements for the operation of white space devices in the band 470–790 MHz. Electronic Communications Committee (2013)
7. Mesodiakaki, A., Adelantado, F., Alonso, L., Verikoukis, C.: Energy-efficient contention-aware channel selection in cognitive radio ad-hoc networks. In: IEEE CAMAD 2012 (2012)
8. Yucek, T., Arslan, H.: A survey of spectrum sensing algorithms for cognitive radio applications. IEEE Commun. Surv. Tutor. **11**(1), 116–130 (2009)
9. Wang, B., Liu, K.J.R.: Advances in cognitive radio networks: a survey. IEEE J. Sel. Topics Signal Process. **5**(1):5–23 (2011)
10. Lunden, J., Koivunen, V., Huttunen, A., Poor, H.V.: Collaborative cyclostationary spectrum sensing for cognitive radio systems. IEEE Trans. Signal Process. **57**(11), 4182–4195 (2009)
11. Zhao, Y., Song, M., Xin, C.: FMAC: A fair MAC protocol for coexisting cognitive radio networks. In: IEEE INFOCOM 2013 (2013)
12. Zhao, Y., Song, M., Xin, C., Wadhwa, M.: Spectrum sensing based on three-state model to accomplish all-level fairness for co-existing multiple cognitive radio networks. In: IEEE INFOCOM 2012 (2013)
13. Mesodiakaki, A., Adelantado, F., Alonso, L., Verikoukis, C.: Fairness Evaluation of a Secondary Network Coexistence Scheme. In: IEEE CAMAD 2013 (2013)
14. Jain, R., et al: A quantitative measure of fairness and discrimination for resource allocation in shared computer systems. Technical Report TR-301, Digital Equipment Corp (1984)
15. Cesana, M., Cuomo, F., Ekici, E.: Routing in cognitive radio networks: challenges and solutions. Ad Hoc Netw. **9**(3), 228–248 (2011)
16. Akyildiz, I.F., Lee, W.Y., Chowdhury, K.R.: Crahns: cognitive radio ad hoc networks. Ad Hoc Netw. **7**(5), 810–836 (2009)
17. A. Akhtar et al., "Multi-hop Cognitive Radio Networking through Beamformed Underlay Secondary Access," IEEE ICC 2012, Ottawa, Ontario, Canada, June 2012
18. Akhtar, M., Holland, O., Le, T., Nakhai, M.R., Aghvami, A.H.: Cooperative cognitive radio beamforming in the presence of location errors. In: IEEE 73rd Vehicular Technology Conference (VTC 2011-Spring), May 2011
19. Mihovska, A., Meucci, F., Prasad, N.R., Cabral, O., Velez, F.J.: Multi-operator resource sharing scenario in the context of imt-advanced systems (invited paper). In: Proceedind of

Layout: T1 Standard SC | Book ID: 318863_1_En | Book ISBN: 978-3-319-04021-9
Chapter No.: 3 | Date: 24-12-2013 | Page: 59/60

Second International Workshop on Cognitive Radio and Advanced Spectrum Management (2009 -CogART 2009), Aalborg, Denmark, May 2009
20. Kellerer, H., Pferschy, U., Pisinger, D.: Knapsack Problems. Springer, Berlin (2005) ISBN 3-540-40286-1
21. Karlof, J.K.: Integer Programming: Theory and Practice. 1st edn. CRC, New York (2005)
22. Monteiro, V., Rodriguez, J., Gameiro, A., Cabral, O., Velez, F.: RAT and cell selection based on load suitability. Invited paper in Proceeding of VTC2008 The 68th IEEE Vehicular Technology Conference, Calgary, Canada (2008)
23. Holma, H., Toskala, A.: WCDMA for UMTS—HSPA evolution and LTE. 1st edn. Wiley, West Sussex, England (2007)
24. TR25.211. Physical channels and mapping of transport channels onto physical channels (FDD), 5th. edn. 3GPP. (2005)
25. Chen, K.-C., Roberto, J., de Marca, B.: Mobile WiMAX, 1st edn. Wiley, West Sussex (2008)
26. 3GPP TR 25.892 v6.0.0, Feasibility Study for Orthogonal Frequency Division Multiplexing (OFDM) for UTRAN enhancement: The 3rd. Generation Partnership Project. Technical Specification Group Radio Access Network (2004)
27. Salo, J., Nur-Alam, M., Chang, K.: Practical Introduction to LTE Radio Planning [Online]. Available: http://www.eceltd.com/lte_rf_wp_02Nov2010.pdf (2010)
28. Vodafone UK Corporate Responsibility Report 2009-10: http://www.vodafone.com/content/dam/vodafone/UK%20CR/downloads/online.pdf (2010). Accessed April 2010
29. 3GPP TR 25825: Technical Specification Group Radio Access Network; Dual-Cell HSDPA Operation. V1.0.0 (2008)
30. Orlando, C., et al.: Integrated common radio resource management with spectrum aggregation over non-contiguous frequency bands. Springer Wireless Pers. Commun. J. February 2011
31. Akyildiz, I., Lee, W., Vuran, M., Mohanty, S.: Next generation/dynamic spectrum access/cognitive radio wireless networks: a survey. Int. J. Comput. Telecommun. Networking **50**(13), 2127–2159 (2006)
32. Yucek, T., Arslan, H.: A survey of spectrum sensing algorithms for cognitive radio applications. IEEE Commun Surv. Tutorials **11**(1), 116–130 (2009)
33. Zhang, J., Zhao, Q., Zou, J.: The IEEE 802.22 WRAN system based on radio environment map (REM). In: Proceedings of First International Workshop on Education, vol. 1, pp. 98–101 (2009)
34. Hossain, E., Niyato, D., Han, Z.: Dynamic Spectrum Access and Management in Cognitive Radio Networks. Cambridge University Press, Cambridge (2009)
35. Arkoulis, S., Kazatzopoulos, L., Delakouridis, C., Marias, G.: Cognitive spectrum and its security issues. In: Proceedings of Next Generation Mobile Applications, Services and Technologies (NGMAST), pp. 565–570 (2008)
36. Parvin, S., Hussain, F.K., Hussain, O.K., Han, S., Tian, B., Chang, E.: Cognitive radio network security: a survey. J. Network Comput. Appl. **35**(6), 1691–1708 (2012)
37. Gibbons, J.D., Chakraborti, S.: Nonparametric Statistical Inference. CRC Press, Boca Raton (2003)
38. Conover, W.J.: Practical nonparametric statistics. Wiley, New York (1998)
39. Zhao, Y. et al.: Performance evaluation of radio environment map enabled cognitive spectrum-sharing networks. IEEE MILCOM 2007, Orlando, Florida (2007)
40. Atanasovski, V., van de Beek, J., Dejonghe, A., Denkovski, D., Gavrilovska, L., Grimoud, S., Mahonen, P., Pavloski, M., Rakovic, V. Riihijarvi, J., Sayrac, B.: Constructing Radio Environment Maps with Heterogeneous Spectrum Sensors. IEEE DySPAN 2011, Aachen, Germany (2011)
41. Denkovski, D., Rakovic, V., Pavloski, M., Chomu, K., Atanasovski, V., Gavrilovska, L.: Integration of Heterogeneous Spectrum Sensing Devices Towards Accurate REM Construction. IEEE WCNC, France (2012)

AQ5

42. Denkovski, D., Atanasovski, V., Gavrilovska, L., Riihijarvi, J., Mahonen, P.: Reliability of a Radio Environment Map: Case of Spatial Interpolation Techniques. CrownCom, Stockholm (2012)
43. EC FP7-248351 project FARAMIR. Deliverable D6.2: Prototype Description and Field Trial Results. Information. http://www.ict-faramir.eu/fileadmin/user_upload/deliverables/FARAMIR-D6.2-Final.pdf
44. EC FP7-248303 project QUASAR. Deliverable 2.2: Methodology for assessing secondary spectrum usage opportunities – final report. Information. http://quasarspectrum.eu/images/stories/Documents/deliverables/QUASAR_D2.2.pdf
45. EC FP7- 248351 project FARAMIR. http://www.ict-faramir.eu/
46. Gavrilovska, L., Atanasovski, V.: Dynamic REM towards flexible spectrum management. 11th International Conference IEEE TELSIKS, Nis, Serbia (2013). Accessed 16–19 Oct 2013
47. Gavrilovska, L., Atanasovski, V., Rakovic, V., Denkovski, D., Angjelicinoski, M.: REM-enabled transmitter localization for ad-hoc scenarios. IEEE MILCOM, San Diego (2013). 17–20 Nov 2013
48. www.fub.it
49. ECC Spectrum Engineering Working Group SE43: Cognitive Radio Systems—White Spaces. http://www.cept.org/ecc/groups/ecc/wg-se/se-43
50. ECC Report 159: Technical and operational requirements for the possible operation of Cognitive Radio Systems in the 'White Space' of the frequency band 470–790 MHz
51. Barbiroli, M., Carciofi, C., Guiducci, D., Petrini, V.: White Spaces potentially available in Italian scenarios based on the geo-location database approach. DySPAN (2012)
52. ITU, Recommendation ITU-R P.1546-2: Method for point-to-area predictions for terrestrial services in the frequency range 30 MHz to 3000 MHz. Ottobre (2009)
53. Karimi H.R.: Geo-location databases for white space devices in the UHF TV bands: Specification of maximum permitted emission levels. In: IEEE Symposium on New Frontiers in Dynamic Spectrum Access Networks (DySPAN 2011)
54. Petrini, V., Karimi, H.R.; TV white space database: Algorithms for the calculation of maximum permitted radiated power levels. ySPAN (2012)
55. ITU: Final Acts of Geneva (2006)
56. Mishra, M., Sahai, A.: How Much White Space Is There?" Technical Report UCB/EECS-2009-3, Electrical Eng. and Computer Sciences Department Univercity of California, Berkeley. http://www.eecs.berkeley.edu/Pubs/TechRpts/2009/EECS-2009-3.html (2009)
57. Van de Beek, J., Riihijarvi, J., Achtzehn, A., Mahonen, P.: TV White Space in Europe. IEEE Trans. Mobile Comput. **11**(2):178–188
58. ITU- R Recommendation P.526: Propagation by diffraction. Approved in 2012-02
59. Harrison, K., Mishra, S., Sahai, A.: How much white-space capacity is there? In: Proceedings IEEE Symposium New Frontiers in Dynamic Spectrum Access Networks (DySPAN'10) (2010)

Author Query Form

Book ID :	**318863_1_En**
Chapter No.:	**3**

Springer
the language of science

Please ensure you fill out your response to the queries raised below and return this form along with your corrections

Dear Author
During the process of typesetting your chapter, the following queries have arisen. Please check your typeset proof carefully against the queries listed below and mark the necessary changes either directly on the proof/online grid or in the 'Author's response' area provided below

Query Refs.	Details Required	Author's Response
AQ1	Please check and confirm that the authors and their respective affiliations have been correctly identified and also confirm corresponding author is correctly identified and amend if necessary.	
AQ2	Please provide a clear text in Fig. 3.9.	
AQ3	Please confirm the section headings are correctly identified.	
AQ4	Please provide the opening paranthesis for the closing paranthesis given in the sentence 'or the allocation of the users'.	
AQ5	Please provide complete details for Ref. [30].	

MARKED PROOF

Please correct and return this set

Please use the proof correction marks shown below for all alterations and corrections. If you wish to return your proof by fax you should ensure that all amendments are written clearly in dark ink and are made well within the page margins.

Instruction to printer	*Textual mark*	*Marginal mark*
Leave unchanged	··· under matter to remain	
Insert in text the matter indicated in the margin		New matter followed by or
Delete	through single character, rule or underline or through all characters to be deleted	or
Substitute character or substitute part of one or more word(s)	through letter or through characters	new character or new characters
Change to italics	under matter to be changed	
Change to capitals	under matter to be changed	
Change to small capitals	under matter to be changed	
Change to bold type	under matter to be changed	
Change to bold italic	under matter to be changed	
Change to lower case	Encircle matter to be changed	
Change italic to upright type	(As above)	
Change bold to non-bold type	(As above)	
Insert 'superior' character	through character or where required	or under character e.g. or
Insert 'inferior' character	(As above)	over character e.g.
Insert full stop	(As above)	
Insert comma	(As above)	
Insert single quotation marks	(As above)	or and/or or
Insert double quotation marks	(As above)	or and/or or
Insert hyphen	(As above)	
Start new paragraph		
No new paragraph		
Transpose		
Close up	linking characters	
Insert or substitute space between characters or words	through character or where required	
Reduce space between characters or words	between characters or words affected	